REPUBLIC OF TURKEY

BEGÜM BİLGE

ACIBADEM MEHMET ALI AYDINLAR UNIVERSITY

INSTITUTE OF HEALTH SCIENCE

MASTER THESIS

ISTANBUL-2018

REPUBLIC OF TURKEY
ACIBADEM MEHMET ALİ AYDINLAR UNIVERSITY
INSTITUTE OF HEALTH SCIENCES

THE EFFECTS OF CYTIDINE-5'-DIPHOSPHOCHOLINE (CDP-CHOLINE) ON AUTOPHAGY AND MITOCHONDRIAL DYNAMICS IN $A\beta_{1-42}$ TREATED PC12 CELLS

BEGÜM BİLGE

MASTER THESIS

MEDICAL BIOTECHNOLOGY PROGRAM

SUPERVISOR

Assoc. Prof. Devrim Öz Arslan

ISTANBUL-2018

REPUBLIC OF TURKEY
ACIBADEM MEHMET ALİ AYDINLAR UNIVERSITY
INSTITUTE OF HEALTH SCIENCES

THE EFFECTS OF CYTIDINE-5'-DIPHOSPHOCHOLINE (CDP-CHOLINE) ON AUTOPHAGY AND MITOCHONDRIAL DYNAMICS IN $A\beta_{1-42}$ TREATED PC12 CELLS

BEGÜM BİLGE

MASTER THESIS

MEDICAL BIOTECHNOLOGY PROGRAM

SUPERVISOR

Assoc. Prof. Devrim Öz Arslan

ISTANBUL-2018

Program: Medical Biotechnology

Title of Thesis: The Effects of Cytidine-5'-Diphosphocholine (CDP-Choline) On Autophagy And Mitochondrial Dynamics in Aβ1-42 Treated PC12 Cells

Student Name and Surname: Begüm Bilge

Date:14/09/2018

This is to certify that I have examined this copy of master thesis. I have found that she prepared after fulfilling requirements specified in the associated legislations before the final examining committee whose signatures are below.

Committee Members

Assoc. Prof. Devrim Öz Arslan (Advisor) ----------

Prof. Beki Kan ----------

Assoc. Prof. Elif Damla Arısan ----------

This thesis has been approved by the above jury and It has been accepted by decision of Health Sciences Board of Directors.

Prof. Uğur Özbek

Director of Health Sciences Institute

DECLARATION

I hereby declare that, this thesis has been written by me based on the data obtained in line with the scientific rules and ethical principles of responsible conduct of research. All information, data, comments, analyses have been collected and processed through scientific, academic writing style, and literature used have been duly shown by giving reference to the original sources in accordance with the publication ethics. I also announce and emphasize that I have not violated any rules secured by patent and copyrights whilst the conduct and writing of this research.

Name, Last name: Begüm Bilge

Signature:

ACKNOWLEDGEMENTS

First and foremost, I would like to thank my supervisor, Assoc. Prof. Devrim Öz Arslan, for her time, patience, guidance and for giving me the opportunity to learn many things in her lab. I am also immensely grateful to Prof. Beki Kan and to Prof. İsmail Hakkı Ulus for their contributions and teachings during the project. I would also like to thank Assoc. Prof. Zeynep Durer and Asst. Prof. Deniz Yücel for their suggestions and helps throughout this project.

My gratitude also goes out to all my colleagues; Tuğçe Demir, Hazal Gezmiş, Süleyman Bozkurt, Berna Üstüner and Gülen Kılıçkaya; who supported and helped me through the good times and the bad. My appreciation also goes to Görkem Gün and other members of Acibadem Mehmet Ali Aydinlar University research laboratories.

I would like to thank warmly to my parents for their endless support and wise counsels.

I would also like to thank to Acibadem Mehmet Ali Aydinlar University for providing laboratory facilities and to Scientific and Technological Research Council of Turkey (TUBITAK) for their financial support. I would also like to thank to SEM Laboratuar Cihazları Paz. San. Ve Tic. A.Ş. for renting us Seahorse XFp Analyzer for our experiments.

This study was supported by TUBITAK 1001 project (114Z494); I was supported as a fellow from 2016 to 2017.

TABLE OF CONTENTS

ABBREVIATIONS

3-MA : 3-metyladenine

a7nAChRs : a7-nicotinic-acetylcholine receptors

α-synuclein : alpha-synuclein

Aβ : Amyloid-beta

Acetyl-CoA : Acetyl coenzyme A

ACh : Acetylcholine

AD : Alzheimer's disease

ADP : Adenosine diphosphate

AFM : Atomic force microscopy

AICD : Amyloid precursor protein intracellular domain

AMBRA1 : Activating molecule in Beclin-1-regulated autophagy

APP : Amyloid precursor protein

APS : Ammonium persulfate

ATG : Autophagy related

ATP : Adenosine triphosphate

AV : Autophagic vacuole

BNIP3 : Bcl2 interacting protein 3

BSA : Bovine serum albumin

Ca^{+2} : Calcium

CCCP : Carbonyl cyanide m-chlorophenyl hydrazone

CDP-Choline : Cytidine-5'-diphosphocholine

CL : Cardiolipin

CMA : Chaperone-mediated autophagy

CNS : Central nervous system

CO_2 : Carbondioxide

CTF α : C-terminal fragment alpha

CTF β **:** C-terminal fragment beta

d **:** days

DAG **:** Diacylglycerol

DAPI **:** 4′, 6-diamidino-2-phenylindole

ddH_2O **:** doubled distilled water

DMSO **:** Dimethylsulfoxide

DNA **:** Deoxyribonucleic acid

Drp1 **:** Dynamin related protein 1

DTT **:** Dithiothreitol

EDTA : Ethylenediaminetetraacetic acid

ER **:** Endoplasmic reticulum

ETC **:** Electron transport chain

FAD **:** Flavine adenine dinucleotide

FCCP **:** Trifluoromethoxy carbonyl cyanide phenyl hydrazone

FIP200 **:** FAK family kinase-interacting protein of 200 kDa

Fis1 **:** Mitochondrial fission 1 protein

FUND1 **:** Fun14 domain-containing protein 1

GABARAP **:** Gamma-aminobutyric acid receptor-associated protein

h **:** hours

HD **:** Huntington disease

H_2O **:** Water

H_2O_2 **:** Hydrogen peroxide

Hsc70 **:** Heat shock-cognate protein of 70kDa

kDa **:** Kilodalton

LC3B **:** Microtubule-associated protein 1A/1B-light chain 3 B

LDH **:** Lactate dehydrogenase

LIR **:** LC3-interacting region

LRRK2 **:** Leucine-rich repeat kinase 2

M **:** Molar

MAM **:** Mitochondria associated membrane

Mff **:** Mitochondria fission factor

Mfn1/2 **:** Mitochondrial fusion 1/2

µg **:** Microgram

min **:** Minutes

MIM **:** Mitochondrial inner membrane

µl **:** Microliter

µM **:** Micromolar

MMP **:** Mitochondrial membrane potential

MOM **:** Mitochondrial outer membrane

mtDNA **:** Mitochondrial DNA

mTOR **:** Mammalian target of rapamycin

mTORC1 **:** Mammalian target of rapamycin complex 1

MTT **:** 3-(4,5-Dimethylethiazol-2-yl)-2,5-Diphenyltetrazolium Bromide

NAD **:** Nicotinamide dinucleotide

NBR1 **:** Neighbor of BRCA1 gene 1

NDP52 **:** Nuclear dot 52kDa protein

NF-κB **:** Nuclear factor kappa B

NFT **:** Neurofibrillary tangle

ng **:** nanogram

NGF **:** Nerve growth factor

nM **:** nanomolar

nm **:** nanometer

NSCs **:** Neuronal stem cells

OCR **:** Oxygen consumption rate

Opa1 **:** Optic atrophy type 1 protein

OXPHOS **:** Oxidative phoshorylation

O_2 **:** Oxygen

O_2^- **:** Superoxide radical

OPTN **:** Optineurin protein

P-UB **:** Polyubiquitinated

PA **:** Phosphatidic acid

PAS **:** Phagophore assembly site

PBS **:** Phosphate-buffered saline

PBST **:** Phosphate-buffered saline Tween

PC **:** Phosphatidylcholine

PC12 **:** Pheochromocytoma

PD **:** Parkinson disease

PE **:** Phosphatidylethanolamine

pH **:** Power of hydrogen

PI **:** Phosphatidylinositol

PI3K **:** Phosphatidylinositol-3-kinase

PINK1 **:** PTEN-induced putative kinase 1

PMSF **:** Phenylmethylsulfonyl fluoride

PS **:** Phosphatidylserine

PS1 **:** Presenilin 1 protein

PVDF **:** Polyvinylidene fluoride

ROS **:** Reactive oxygen species

RIPA **:** Radioimmunoprecipitation assay

sAPP α/β **:** Soluble APP alpha/beta

SDS **:** Sodium dodecylsulfate

SDS-PAGE **:** SDS polyacrylamide gel electrophoresis

SNARE **:**Soluble N-ethylmaleimide-sensitive factor activating protein receptor

TAX1BP1 : Tax-1 binding protein 1

TEM **:** Transmission electron microscope

TEMED **:** Tetramethylethylenediamine

ULK1 **:** Unc-51 like autophagy activating kinase 1

UPS **:** Ubiquitine proteasome system

UVRAG **:** UV radiation resistance associated gene protein

vATPase **:** Vacuolar-type H^+-ATPase

LIST OF TABLES AND FIGURES

SUMMARY

The Effects of Cytidine-5'-Diphosphocholine (CDP-Choline) on Autophagy and Mitochondrial Dynamics in $A\beta_{1-42}$ Treated PC12 Cells

Recent studies suggest that autophagy may have a crucial role in Alzheimer's disease (AD). Cytidine-5'-diphosphocholine (CDP-Choline), an intermediate in the biosyntesis of membrane phospholipids, is known to have neuroprotective effects in several diseases but the mechanism remains unclear. In this study, the effects of CDP-Choline on autophagy and mitochondrial dynamics were investigated during amyloid-beta ($A\beta_{1-42}$) mediated neuronal injury. For this purpose, PC12 cells were differentiated with nerve growth factor (NGF), followed with $A\beta_{1-42}$ treatment in the presence and absence of CDP-Choline. Autophagy proteins, LC3B, p62 and Beclin-1, and mitochondrial Mitofusin-2 levels were analysed by western blotting. MMP, mitochondrial superoxide and mitochondrial mass were evaluated by flow cytometry and confocal imaging after probing with MitoTracker Red CMXRos, MitoSox and MitoTracker Green FM, respectively. Oxygen consumption rate (OCR) was measured by Seahorse XFP Cell Mito Stress Kit. Results revealed an increase in LC3B and Mitofusin-2 levels of differentiated PC12 cells upon CDP-Choline treatment. Similarly, $A\beta_{1-42}$-treated cells showed increased LC3B, BECN1 and Mitofusin-2 levels. Although CDP-Choline treatment did not cause any change in MMP; mitochondrial mass and mitochondrial superoxide formation were increased. In addition, mitochondrial respiration was reduced in CDP-Choline treated PC12 cells. Furthermore, an increase in MMP levels was observed following 12.5μM $A\beta_{1-42}$ treatment. Moreover, CDP-Choline pre-treatment resulted in decreased MitoSox levels in PC12 cells treated with higher $A\beta_{1-42}$ concentrations. Hence, potential neuroprotective effect of CDP-Choline by altering mitochondrial dynamics and autophagic flux was proposed. This work may contribute to the design of new therapeutic strategies for treatment of neurodegenerative diseases.

Keywords: Alzheimer's Disease, autophagy, CDP-Choline, mitochondria, neurodegeneration

ÖZET

$A\beta_{1-42}$ hasarına uğramış PC12 hücrelerinde Sitidin-5'-difosfokolin'in (CDP-Kolin) otofaji ve mitokondriyel dinamiklere etkisi

Son çalışmalar Alzheimer hastalığında (AH) otofajinin önemli bir rolü olabileceğini düşündürmektedir. Sitidin-5'-difosfokolin (CDP-Kolin)'in membran fosfolipid biyosentezinde bir ara ürün olarak çeşitli hastalıklarda koruyucu etkisinin olduğu bilinmesine rağmen, mekanizması belirsizdir. Bu çalışmada, $A\beta_{1-42}$ hasarına uğrayan hücrelerde CDP-Kolin'in otofaji ve mitokondri dinamiklerine etkisi incelenmiştir. Bu amaçla, PC12 hücreleri NGF ile farklılaştırıldıktan sonra CDP-Kolin varlığında ve yokluğunda $A\beta_{1-42}$ ile muamele edildi. Otofaji proteinlerinden LC3B, p62 ve Beclin-1 ile mitokondriyel Mitofusin-2 seviyeleri western blot ile analiz edildi. MMP, mitokondriyel süperoksit miktari ve mitokondriyel kütle değişimi sırası ile MitoTracker Red CMXRos, MitoSox ve MitoTracker Green FM boyaları kullanılarak akış sitometri ve konfokal mikroskopi ile incelendi. Ayrıca oksijen tüketim oranı Seahore XFp Cell Mito Stress kiti kullanılarak ölçüldü. CDP-Kolin uygulaması LC3B ve Mitofusin-2 seviyelerini arttırmıştır. Aynı şekilde, $A\beta_{1-42}$ ile muamele edilen PC12 hücrelerinde LC3B, BECN1 ve Mitofusin-2 seviyelerinde artış görülmüştür. CDP-Kolin uygulaması MMP'de bir değişime yol açmazken MitoSox ve mitokondriyel kütlede artışa neden olmuştur. Ayrıca, CDP-Kolin uygulanan hücrelerde mitokondriyel solunum azalmıştır. Bunun dışında, 12.5µM $A\beta_{1-42}$ MMP seviyesinde artışa neden olmuştur. Bunlara ek olarak, daha yüksek $A\beta_{1-42}$ ile muamele edilen PC12 hücrelerinde CDP-Kolin ön uygulaması MitoSox seviyelerinde düşüşe sebep olmuştur. Dolayısı ile CDP-Kolin'in nöronlar üzerinde otofaji mekanizmasını ve mitokondriyel dinamikleri değiştirerek bir koruyucu etki yarattığı önerilmiştir. Bu çalışma nörodejeneratif hastalıkların tedavisinde kullanılabilecek yeni stratejilerin bulunmasına yardımcı olabilir.

Anahtar Sözcükler: Alzheimer hastalığı, CDP-Kolin, mitokondri, nörodejenerasyon, otofaji

BACKGROUND AND AIM OF THE STUDY

Autophagy is a highly conserved and important mechanism involved in maintaining cellular homeostasis by degrading aggregate-prone toxic molecules, long lived or damaged proteins and organelles into their building blocks for reuse. Autophagy functions at basal levels in different cellular types but mostly it is considered as an adaptive process induced by several stress conditions including nutrient starvation, growth factor reduction, hypoxia and infection. Three different forms of autophagy have been identified to date, named as macroautophagy, microautophagy and chaperone-mediated autophagy. This study has focused on macroautophagy, referred to as autophagy hereafter. A double membrane structure, named as autophagosome, formation is initiated after autophagy induction to engulf substrates for their degradation following fusion with lysosomes. Several protein complexes and phospholipids are responsible from the proper functioning of autophagy machinery. PE-conjugated LC3, which remains bound to the outer membrane of autophagosome until lysosome degradation, is accepted as the marker protein of autophagy mechanism (12, 123). Membrane origins of autophagosome still remain undetermined, but ER and mitochondria are considered to be the potential precursors since they are responsible from the synthesis of phospholipids like PE, PC and PS. PE was shown to conjugate with LC3 upon synthesis via CDP ethanolamine pathway. Moreover, PC is produced via a similar pathway involving choline and DAG (34). However, the role of PC in autophagosome formation is not known. Similarly, mitochondria play an important role in cellular homeostasis by preserving cellular bioenergetics with their highly dynamic structure as they are the main organelles responsible from energy production. Mitochondria are also double membrane structures, which makes their function dependent on phospholipids. In addition, PC is considered as the major constituent of mitochondrial membranes (67). Mitochondrial dynamics are highly regulated with different complex mechanism and damaged mitochondria are degraded via mitophagy, a selective type of autophagy. Hence, the role of cytidine-5’-diphosphocholine (CDP-Choline) in autophagy-related

protein levels and mitochondrial dynamics in differentiated PC12 cells has been the focus of this study.

Autophagy can prevent the aggregation of misfolded proteins and provide neuroprotection against neurodegenerative diseases. However, increased autophagy and mitophagy levels have been observed in neurodegeneration. Hence, whether active autophagy is beneficial in neurodegenerative diseases and if so, the factors involved in this role remain unknown (32, 87). In addition, neuroprotective effects of CDP-Choline has been demonstrated in various CNS-related disorders and is commercially available as a food supply an known in the name of 'citicoline'. The mechanism of this neuroprotection is yet to be discovered (6). We proposed that neuroprotection provided by CDP-Choline treatment might be related to the regulation of autophagic flux and mitochondrial dynamics by supplying necessary PC and other phospholipids involved in autophagosome formation. For this purpose, differentiated PC12 cells will be incubated with CDP-Choline and $A\beta_{1-42}$ injury, commonly used in the constitution of Alzheimer's disease model, will be applied in the presence and the absence of autophagy inducer and inhibitors. Therefore, the possible role of pre-treatment with CDP-Choline in autophagy and mitochondrial dynamics will be investigated in $A\beta_{1-42}$ injured PC12 cells.

1.INTRODUCTION

1.1. Autophagy

In eukaryotic cells, two major degradation pathways are responsible from maintaining cellular homeostasis. One of them is ubiquitin-proteasome system (UPS), which is responsible from degrading most of the short-lived and damaged proteins. The other pathway is autophagic pathway, in which long-lived proteins and organelles are degraded into their building blocks (60, 11).

Autophagy, which is derived from Latin, means ‘self-eating and is a highly conserved dynamic mechanism. In this mechanism, cytoplasmic contents, such as proteins, lipids, organelles are delivered to lysosome for degradation to preserve cellular homeostasis. Under normal conditions, autophagy occurs at low levels, but it is induced by several stimuli like starvation, damaged organelles, aggregated proteins, DNA damage and infection (76, 94, 119). Autophagy can be named according to the cargo to be degraded. For example the degradation of the ER can be named as ER-phagy or reticulophagy, mitochondria as mitophagy, ribosomes as ribophagy, peroxisomes as pexophagy, lipid droplets as lipophagy, pathogens as xenophagy and aggregated proteins as aggrephagy (111).

Three distinct forms of autophagy have been identified; macroautophagy, microautophagy and chaperone-mediated autophagy (CMA). The common features of these three types of autophagy are to recycle the building blocks of the degraded substrates to maintain cellular homeostasis. In microautophagy, the cargo to be degraded is invaginated by the lysosomal membrane. The vesicle containing the cargo goes inside the lumen of the lysosome and is degraded. This degradation can be in a selective manner or ‘in bulk’, which refers to non-selective manner (111).

In chaperone-mediated autophagy (CMA), substrates containing KFERQ motif are recognized by the heat shock-cognate protein of 70KDa (hsc70) and transported to the lysosome for degradation. Different from other types of autophagy, CMA only occurs in a selective manner (24).

The last and the most studied type of autophagy is macroautophagy, simply called autophagy hereafter, consisting of isolating the substrate within a cytosolic double-membrane structure, called autophagosome, and the fusion of autophagosome with lysosome for degradation (29).

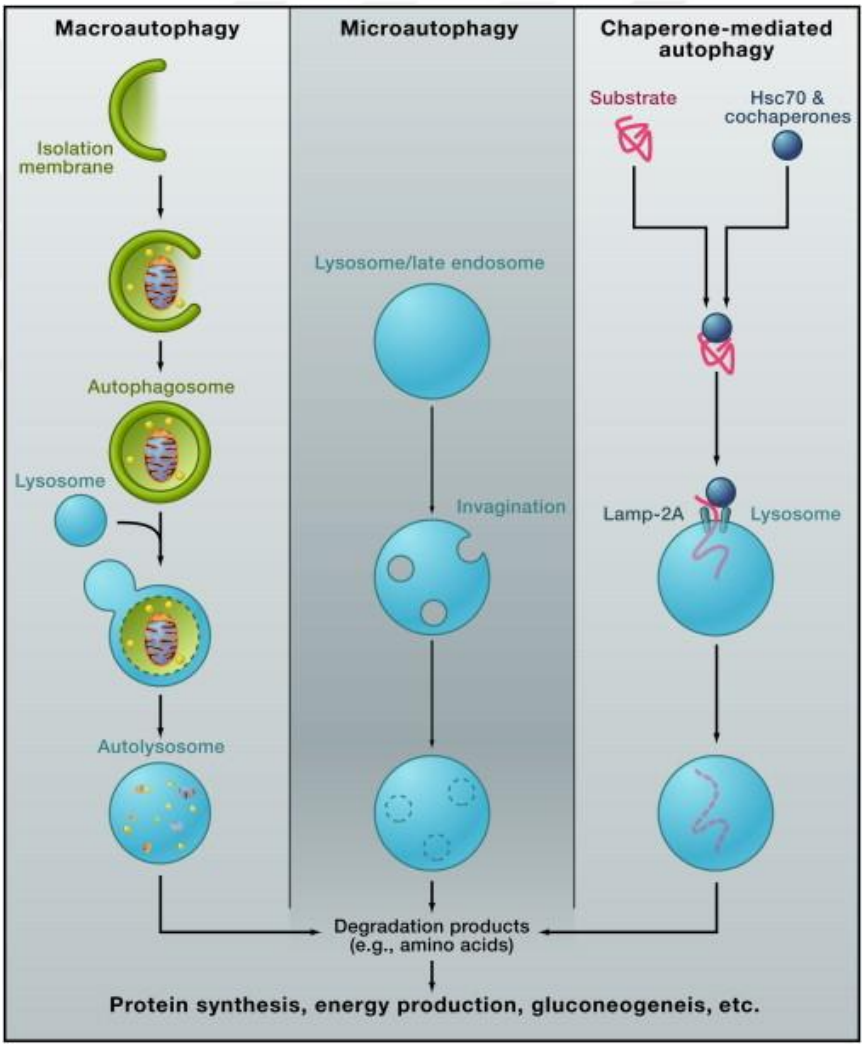

Figure 1. Different types of autophagy (72).

Autophagy is a highly regulated and dynamic mechanism. Proteins involved in the regulation of autophagy machinery are called autophagy related proteins (ATG) and they have first been identified in yeast. More than 35 ATG proteins are described in yeast, and most of them have homologs in mammals (120). Majority of these ATG proteins are involved in the formation of the autophagosome, which can be divided into four stages: initiation, elongation, maturation and fusion with lysosome and degradation. Autophagosome formation is initiated with a stimulus like amino acid deprivation and begins with the isolation membrane formation, which is specifically called 'phagophore'. Even though the origins of the phagophore still remain unclear, it has been shown that the formation takes place near the endoplasmic reticulum. But, mitochondria, Golgi and plasma membrane are also considered as membrane sources for autophagosome (122). Two protein complexes are active in the initiation step of the autophagosome formation: ULK1 complex, composed of ULK1, ATG13, FIP200 and ATG101 and class III PI3K complex (Beclin1 complex), composed of class III PI3K, VPS34, Beclin1 and ATG14. Under normal conditions, ULK1 complex is phosphorylated by the mammalian target of rapamycin complex 1 (mTORC1). Under stressed conditions; like starvation, growth factor deprivation and decrease in ATP levels; ULK1 complex is activated and phosphorylates class III PI3K complex. Both complexes trigger the nucleation of the phagophore and the accumulation of other ATG proteins to the phagophore assembly site (PAS). Two ubiquitin-like conjugation systems are responsible from the elongation phase of the autophagosome: ATG12-5-16 conjugation system and the modification of Atg8 family proteins, which consist of microtubule-associated 1A/1B LC3 (MAP1LC3) subfamily and GABARAP subfamily, with phosphatidylethanolamine. Once the phagophore is formed, ATG5 is conjugated to ATG12 by ATG7 and ATG10, that act like E1 and E2-like enzymes, respectively. Afterwards, ATG12-5 conjugate binds to ATG16L to form the ATG12-5-16 complex. Furthermore, LC3-I is formed by the cleavage of ATG8/LC3 by ATG4,and LC3-I conjugates to phosphatidylethanolamine (PE) accompanied by ATG7 and ATG3. This conjugation results in the formation of LC3-II, which remains bound to the inner and the outer membrane of the autophagosome until it fuses with lysosome (27, 29, 74, 118, 119). Therefore LC3-II becomes the most practical marker to monitor autophagic activity (99,119). These

two ubiquitin-like conjugation systems responsible from the elongation of the autophagosome are demonstrated to be connected to each other as well. Sou et al. (96) showed that the ATG12-5 conjugation is decreased in ATG3 deficient mice. On the other hand, Fujita et al. (31) demonstrated that the proper functioning of ATG5-12-16 complex is required for the proper lipidation of LC3. After closure of the double membrane structure, ATG5-12-16 complex dissociates from the autophagosome membrane and the transfer of the autophagosome containing the cytoplasmic content to be degraded along microtubules to lysosome is accomplished by the help of motor proteins like dynein and kinesin (76). Autophagosome firstly fuses with an endosome to form the amphisome, then fuses with lysosome to form autophagolysosome or autolysosome (71). This fusion is highly regulated by several membrane protein complexes, such as SNAREs (27). After fusion with lysosome, the cargo content within the inner membrane of the autophagosome is degraded with hydrolases. This degradation process depends on the acidity of the lysosome, which is regulated by presenilin1 (PS1) and the vATPase proton pump. Once the content is degraded, its building blocks such as amino acids are released back into the cytoplasm with the help of ATG proteins (121)

This highly regulated and complex mechanism has roles in cell growth, cell survival and cell death. Therefore, alterations in this mechanism and mutations in Atg genes is associated with diseases such as neurodegenerative disorders, cancer, infectious diseases, metabolic disorders and autoimmune diseases (104).

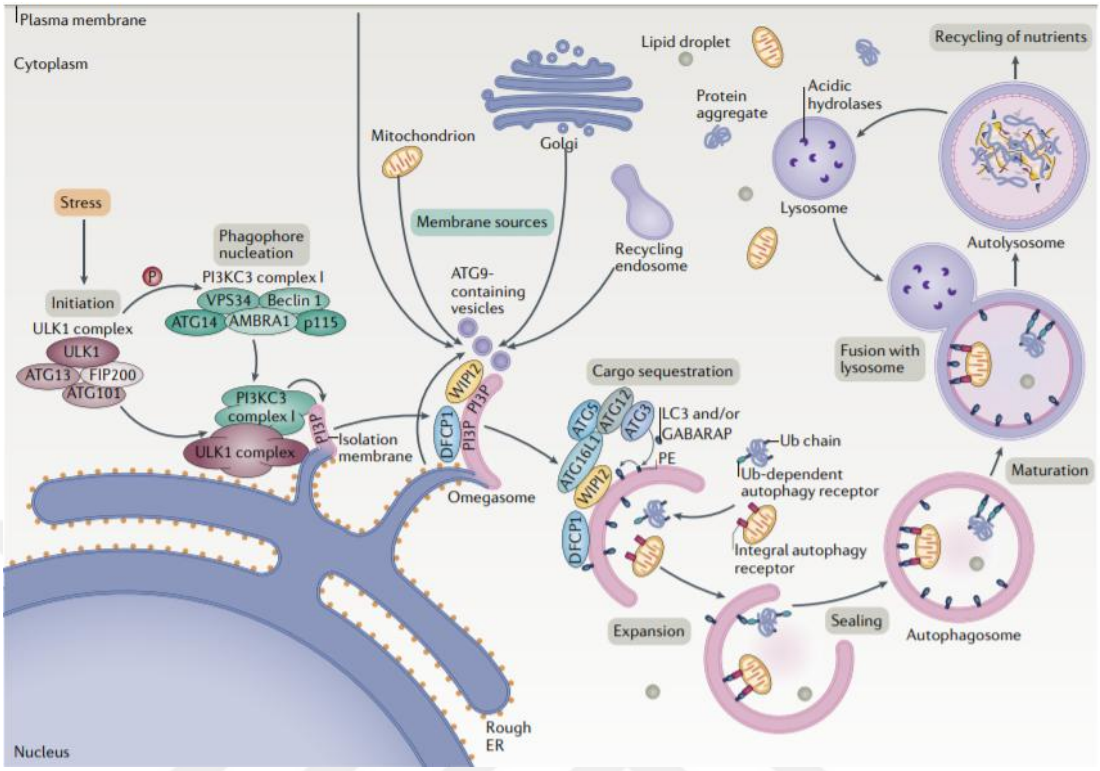

Figure 2. Overview of the autophagy mechanism (27).

1.1.1. Regulation of autophagy

Autophagy mechanism is controlled by several signaling pathways. These pathways can be categorized into two groups: mTOR-dependent and mTOR-independent controlling pathways. mTOR-dependent regulation of autophagy is considered to be the classical regulator of autophagy machinery, in which mTORC1 complex negatively regulates autophagy mechanism. One of the well-known pharmacological inhibitor of mTORC1 complex is rapamycin. On the other hand, mTOR independent regulation of autophagy involves inositol and Beclin-1 signalling pathways. Increased inositol levels inhibit autophagosome formation and drugs like lithium that lower inositol levels induce autophagic activity, independent of the mTOR signaling pathway (88). Also more recently, Manzoni et al. (64) demonstrated that, independent from canonical regulation of autophagy by mTOR signaling, inhibiton of LRRK2, whose genetic mutation is considered as the major reason of

familial Parkinson's disease, increases cellular autophagy levels by directly increasing the activity of Beclin-1 complex.

1.2. Lipids and Autophagy

Lipids have structural and biosynthetic features with their hydrophobic, sometimes amphipathic organizations. Thus far, more than thousand different lipids have been identified in eukaryotes and they can be divided into eight groups according to their functional and structural properties, as fatty acids, glycerolipids, glycerophospholipids, sphingolipids, sterol lipids, phenol lipids, saccharolipids and polyketides. We will focus on phospholipids, which have both structural and signalling functions. Phosphatidylcholine (PC), phosphatdylinositol (PI), phoaphatdylethanolamine (PE), phosphatidic acid (PA), phosphatidylserine (PS) and phosphatidylglycerol (PG) are the members of phospholipids (8). PC and PE are the major constituents of biological membranes, including the plasma membrane, mitochondrial membrane and others. *De novo* synthesis of these phospholipids occurs via the Kennedy pathway, in which substrate specific enzymes, such as choline kinase, ethanolamine kinase, cholinephosphotransferase and ethanolaminephosphotransferase, catalyze the synthesis of PC and PE (34). Phospholipids are important factors in cellular homeostasis and signalling. Hence, any disruption in their profile would result in CNS related disorders and neurodegenerative diseases. Thinner lipid membranes are found in post-mortem brains of AD patients and especially PC and PE levels are lower in AD patients compared to age matched controls (109). These findings are supported by the work of Chadwick et al. (19) demonstrating proteomic changes in the mouse model of AD due to the alterations in lipid rafts. Moreover, phospholipids are crucial for autophagic activity, since they are involved in the formation of autophagosome, a double-membrane structure, and they are also important in the signalling cascade of autophagy. PI and PA have roles in the activation of autophagy machinery. PI activates class III PI3K complex, which is among the central complexes involved in autophagy initiation, and recruits Atg5 to the phagophore. Likewise, PA acts as an activator of autophagy by inhibiting mTOR pathway (93). Phospholipids are also required for phagophore formation. The mitochondria associated membranes

(MAMs), which are the contact site between ER and mitochondria, are putatively considered as the major constituent of phagophore and they are the most important site for lipid synthesis and transport (43). Furthermore, PE is an important determinant for autophagic activity, because lipidation of LC3B with PE is the key reaction for autophagosome elongation (55).

Lipids are also important for mitochondrial homeostasis, which includes mitochondrial fusion and fission events and mitophagy. Some of the lipids, including PE, PA, cardiolipin (CL) and diacylglycerol (DAG) are involved in the control of mitochondrial shape and functions. Hoppins et al. (42) showed that initiation of mitochondrial fusion requires binding of Opa1, which is among the regulators of fusion, to negatively charged phospholipids. In the same way, Abramovici et al. (1) proved the involvement of DAG in mitochondrial fission by showing the dependence of the mitochondrial recruitment of Drp1, one of the proteins involved in fission, on the activity of DAG. Similarly, Mitsuhashi et al. (70) showed that defects in choline kinase, an enzyme essential for the production of PC, resulted in mitochondrial dysfunction in a mouse model of rostrocaudal muscular dystrophy. It is also reported that mitochondrial dysfunction seen in neurodegenerative diseases can be caused by changes in mitochondrial lipid composition (8). For example, disruption in mitochondrial PE levels would result in impaired mitochondrial function, followed by the accumulation of α-synuclein, which is one of the hallmarks of PD (43). Similarly, increased oxidative stress due to excessive ROS production causes lipid peroxidation followed by alterations in mtDNA and mitochondrial proteins and neuronal degeneration.

1.2.1. CDP-Choline

Cytidine-5'-diphosphocholine is intermediate in *de novo* synthesis of PC via Kennedy pathway in which choline is phosphorylated by choline kinase to obtain phosphocholine. Next, phosphocholine assembles with cytidine triphosphate. This reaction is catalyzed by cytidylyl transferase to produce CDP-Choline. Then PC formation is followed upon the combination of CDP-Choline with DAG and omega 3

acid, a reaction catalyzed by phosphocholine transferase. Choline used in this pathway can be obtained via diet or via hydrolysis of PC produced by the methylation of PE catalyzed by hepatic enzymes (115). CDP-Choline is also involved in acetylcholine (ACh) formation, which is a neurotransmitter responsible from motor and cognitive functions of the brain. Wurtman et al. (114) have demonstrated that PC in the membranes are degraded to provide adequate levels of ACh in the absence of choline.

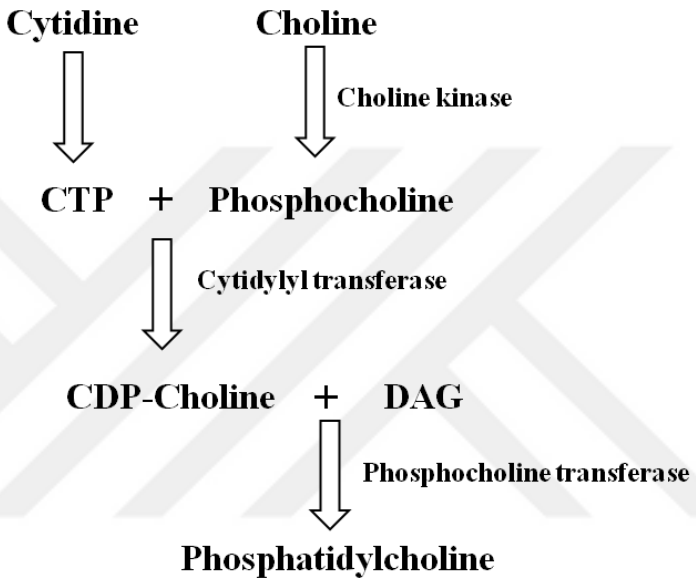

Figure 3. *De novo* synthesis of phosphatidylcholine via Kennedy pathway

CDP-Choline has been used as a neuroprotective or neurorecovery agent in multiple *in vivo* and *in vitro* trials concerning CNS related diseases, such as stroke and traumatic brain injury (TBI); and neurodegenerative diseases like AD. Hence its commercial form is available as an exogenous choline supply in the name of 'citicoline'. It is comprised of ribose, pyrophosphate, cytosine and choline. It can be taken both orally and intravenously, and hydrolyzed into choline and cytidine. Choline is able to pass the blood brain barrier in a concentration-dependent diffusion manner. It is considered to have relatively with fewer adverse effects compared to other drugs used for this purpose (6, 115).

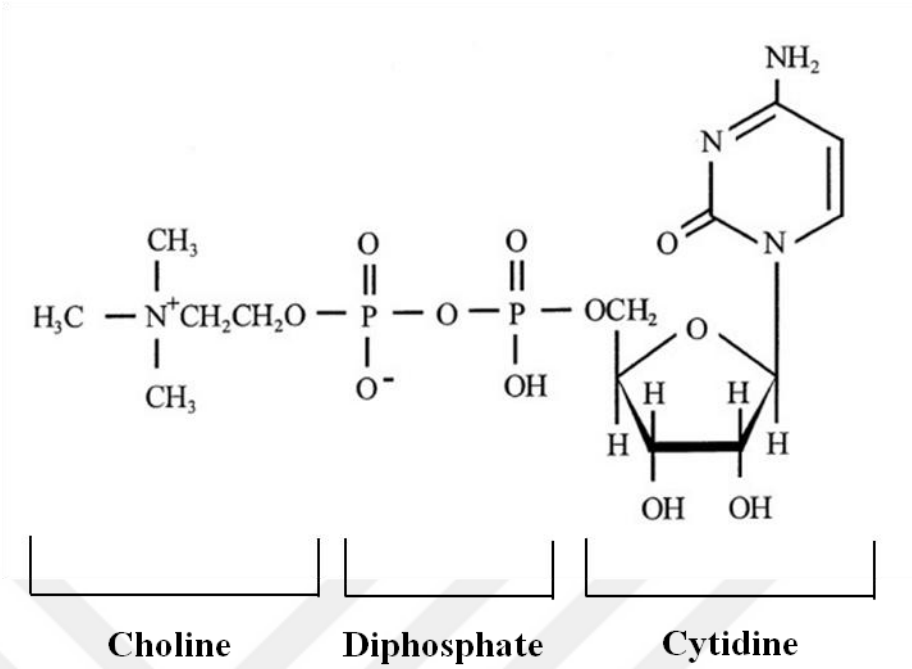

Figure 4. Structure of CDP-Choline

The effects of CDP-Choline on neurorecovery were studied by Dempsey and Raghavendra (25) in a rat model of TBI who showed that CDP-Choline treatment after injury improved neurological function and prevented neuronal loss. Similarly, Guttierez-Fernandez et al. (38) showed that CDP-Choline treatment relieved brain edema and reduced the infracted brain area in a rat model of stroke. CDP-Choline is also suggested as a therapeutic agent in AD by several groups who demonstrated that citicoline enhanced the cognitive deficits in patients with AD (49). There is also evidence for the interactions between toxic Aβ and phospholipids, suggesting that any disruption in membrane phospholipids may trigger the cleavage of APP through the amyloidogenic pathway (108). Therefore, CDP-Choline, as the precursor of PC and other phospholipids, may be used in AD treatment to inhibit toxic Aβ production and to ameliorate synaptic function (115).

As previously described, phospholipid composition and function is important for mitochondrial dynamics. CDP-Choline, in this respect, has effects on mitochondrial lipid composition, brain energy metabolism, synthesis of nucleic acids and mitochondrial protein compositions. Therefore, CDP-Choline constitutes a promising

therapeutic target for the treatment of neurodegenerative diseases by reducing oxidative stress, increasing ACh and dopamine levels and enhancing ATP production (106).

1.3. Neurodegeneration and Autophagy

Neuronal cells differ from the other cells with their specific structure containing soma and neurites. This structure requires proper transport of important macromolecules and organelles, like mitochondria, from soma to neurites and vice versa for maintaining its integrity and function. Any disruption in this structure may form aggregates or may damage organelles. Since neurons are in postmitotic stage, they cannot reduce the damage by cellular division. This is why autophagy plays an important role in the maintainance of neuronal homeostasis as it is the main mechanism for degradation of damaged proteins and organelles (7). Accumulation of aggregated proteins and damaged organelles are the main reasons for neurodegeneration: Alzheimer's disease (AD) is characterized by the formation of amyloid-β plaques. Accumulated Lewy bodies containing mutant α-synuclein cause Parkinson disease (PD) and accumulation of mutant huntingtin protein is the main cause of Huntington disease (HD) (68). Impaired or non-functioning autophagy is considered among the main factors driving these causes of neurodegenerative diseases. Hara et al. and Komatsu et al. (41, 56) showed that suppression of autophagy by silencing ATG5 and ATG7 genes, which are among the most important proteins involved in autophagosome formation, induced accumulation of protein aggregates, neurodegeneration and neuronal loss in mice. Some of the autophagy inducers, like rapamycin and trehalose, are used for enhanced clearance of pathologic proteins in neurodegenerative diseases models (87). However it is still unclear whether induction of autophagy is totally beneficial for neurodegeneration or not, since overactivation of autophagy mechanism results in the accumulation of autophagosomes containing aggregated proteins and in the induction of neuronal cell death (80, 95). Therefore, autophagic flux, composed of the balance between auophagosome formation and its degradation via lysosomal fusion, should be tightly controlled (63).

1.3.1. Alzheimer's disease

Alzheimer's disease (AD) is the most frequent neurodegenerative disease affecting elderly people. AD is characterized by progressive loss of cognitive function and memory loss caused by neuronal degeneration and loss in cerebral cortex and in sub-cortical regions (69). To date, almost 44 million people have been diagnosed with AD, and this number is predicted to increase three times in fifty years. Small proportion of patients possess mutations in one of three genes, presenilin 1 and 2 and amyloid precursor protein, and they form the familial AD subgroup. On the other hand, 95% of AD cases are known as sporadic AD whose causes are still undetermined. Nevertheless, these two types of AD show same neuropathologies including senile plaques composed of aggregated β-amyloid (Aβ) and neurofibrillary tangles (NFTs) consisting of hyperphosphorylated tau (54, 69, 82).

1.3.1.1. Aβ formation

Aβ is produced by sequential cleavage of amyloid precursor protein (APP) which is a transmembrane protein. Two different pathways are defined for APP cleavage according to the toxicity of the end product. The first one is the non-amyloidogenic pathway involved in the production of non-pathogenic fragments. This pathway consists of cleavage of APP with α-secretase to obtain soluble APP α (sAPPα) and membrane-bound C-terminal fragment α (CTFα). CTFα is then cleaved with γ-secretase to release p3 and APP intracellular domain (AICD). The second pathway is amyloidogenic pathway which is primarily responsible from the production of toxic Aβ peptides. In this pathway, APP is cleaved by β-secretase to obtain sAPPβ and CTFβ. Then, CTFβ is cleaved with γ-secretase to release Aβ peptides (26). The length of these Aβ peptides differs from each other, but it can be divided into two groups, as Aβ40 and Aβ42. Aβ40 is the most prevalent product and it is generally responsible from neurite function. On the other hand, Aβ42 formation occurs in small proportion, but it is prone to form aggregates, which are the main constituents of senile plaques (82).

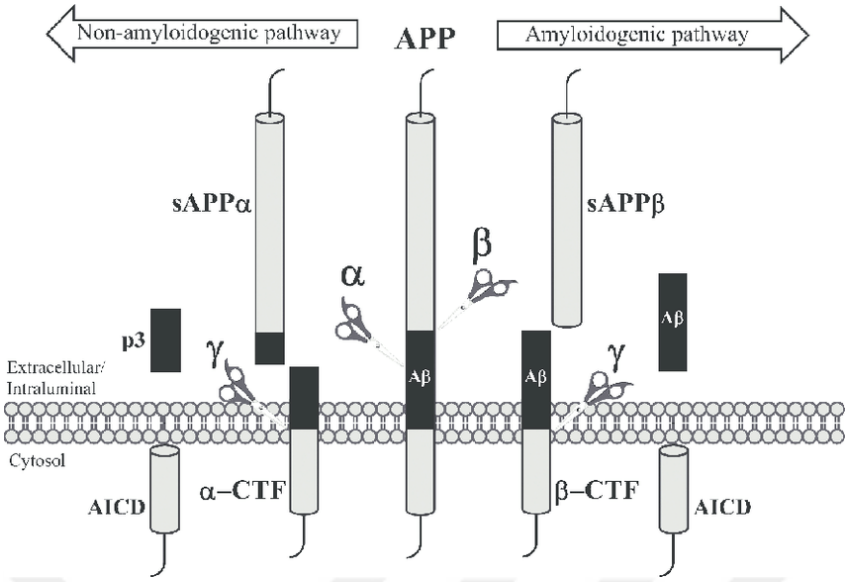

Figure 5. APP cleavage by secretases (75).

1.3.1.2. Tau pathology

Tau is a microtubule associated protein, which mainly localizes in neurons and helps to stabilize microtubules. Tau is indispensible for proper neuronal function because of its high tendency to bind microtubules, which makes it a major factor in tubulin organization and axonal transport of organelles, like mitochondria and lysosomes, and of vesicles in the brain (21).

Formation of intraneuronal neurofibrillary tangles (NFTs) composed of hyperphosphorylated tau protein is the second hallmark for the diagnosis of AD. But before the formation of NFTs, tau protein is subjected to several post-translational modifications, such as truncation, N-glycolysation, acetylation and phosphorylation. These modifications serve to distinguish it from the normal form of tau protein and as such, enable them to be detected decades before the first symptoms of AD (22). As a result of the post-translational modificiations, tau loses its ability to bind to microtubules, and cytosolic tau levels increase. This increase enhances tau-tau interactions and its polymerization and aggregation. Paired helical fragments (PHF) are formed with tau aggregates and initiate the formation of NFTs (47). Furthermore,

a recent study (48) revealed that neurodegeneration and cognitive deficits seen in AD are caused by tau, but not Aβ aggregation. Therefore it is suggested as a therapeutic target for the treatment of neurodegenerative diseases.

1.3.2. Alzheimer's disease and autophagy

The role of autophagy during AD remains controversial, because it is known that autophagy mechanism is induced during the early onset of the disease, however it is also shown that there is an extensive increase in autophagic vacuoles (AV) along the dystrophic neurites in post-mortem brains of AD and *in vitro* AD models (81). Aggregated proteins, like Aβ and tau, accelerate the depolymerisation of microtubules which directly affects autophagic flux. The balance between autophagosome formation and its degradation by fusion with lysosome is defected since the latter is dependent on the axonal transport of autophagosomes along microtubules. Therefore, depolarization of microtubules results in the inhibition of autophagosome-lysosome fusion (111). There is also evidence that autolysosomes are also accumulated in dystrophic neurites along with AVs in AD, which suggests that there is a lysosomal dysfunction causing autophagy failure. An increase in lysosomal pH is suggested as the reason for this impairment, which in turn makes lysosomal hydrolases responsible from the degradation of toxic proteins inactive (112). On the other hand, Yu et al. (125) showed that accumulated AVs are enriched in APP, βCTF and the components of γ-secretase complex, which are mainly responsible from the production of Aβ peptides in AD affected brains and in *in vitro* models of AD. This finding revealed a role for autophagy mechanism in production of Aβ peptides in AD.

1.4. Mitochondria

Mitochondria are known as 'power houses' for eukaryotic cells, since they are responsible from ATP production for cell survival (79). Apart from their role in energy production, mitochondria are also important regulators of ion homeostasis, lipid metabolism and induction of apoptotic cell death (85). Since they originate form bacteria, mitochondria have their own DNA, referred to as mitochondrial DNA (mtDNA) (61). Mitochondria are generally shaped as cylinders with a diameter of

0.5-1μm and they are remarkably mobile and plastic organelles (3). Mitochondria number can vary between hundreds to thousands in different cells, according to the cellular energy demand.

Mitochondria are enclosed by two membranes containing different proteins and having different functions: outer membrane and inner membrane. The area between these two membranes is called the intermembrane space, and the area inside the inner membrane is called the inner matrix. Porin molecules, which form transport channels across the outer membrane make it permeable to ions and small molecules. On the other hand, the transport of small molecules through the inner membrane of mitochondria is only achieved by transport proteins, because, cardiolipin, a phospholipid mostly localized in the mitochondrial inner membrane, makes the mitochondrial inner membrane impermeable to ions and small molecules. The inner membrane of mitochondrion is formed of infoldings, named as 'cristae' whose shape expand the surface area of the membrane to increase the ATP production capacity of the cell (3). Components of the electron transport chain (ETC) and enzymes like ATP synthase and ADP-ATP translocases are situated in the mitochondrial inner membrane, whereas enzymes responsible from citric acid cycle, fatty acid β-oxidation and amino acid oxidation, the pyruvate dehydrogenase complex, mitochondrial DNA, ATP and ADP are located in the mitochondrial matrix (77).

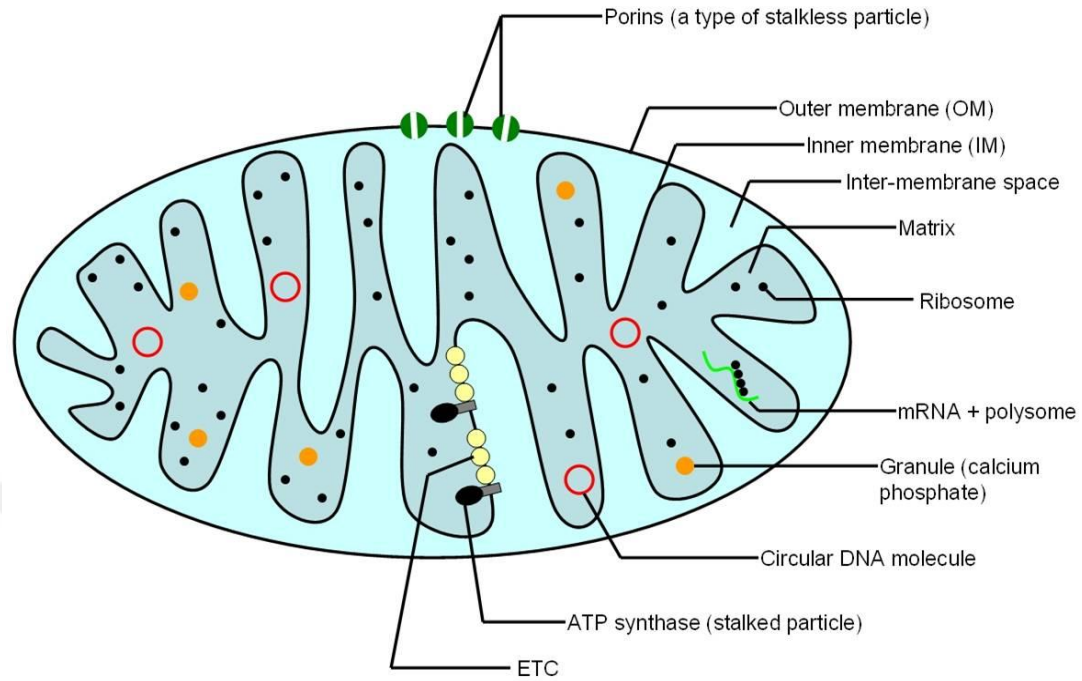

Figure 6. Structure of a mitochondrion (http://cronodon.com/BioTech/Respiration.html, accessed 9th July 2018)

1.4.1. Mitochondrial respiration

Cells degrade complex organic molecules into simpler forms for energy production. This process is also called catabolism, and can occur anaerobically, referred to as fermentation, or aerobically, which is the most common way to produce energy in mitochondria (77). Here, we will mainly focus on aerobic degradation of complex organic molecules, like glucose, which proceeds in three major steps: glycolysis, Krebs cycle and oxidative phosphorylation (OXPHOS). Glycolysis takes place in the cytosol and results in the conversion of one molecule of six-carbon glucose into two molecules of three-carbon pyruvates. Glycolysis occurs within ten steps and each step is catalyzed by a different enzyme. These steps can be divided into two parts. The first part, comprising the phosphorylation of glucose, can be perceived as a preparation step for ATP production. On the other hand, ATP production takes place in the second part of glycolysis by substrate-level

phosphorylation and by the reduction of NAD+ to NADH. As a result, two molecules of ATP and two molecules of NADH are produced at the end of conversion of glucose to two molecules of pyruvate.

Krebs cycle or citric acid cycle mostly takes place in the mitochondrial matrix and the pyruvate molecule obtained from glycolysis is converted into carbondioxide (CO_2). A series of reactions begins with the formation of two-carbon acetyl-CoA from three-carbon pyruvate by the involvement of pyruvate dehydrogenase complex. The energy from this breakdown is captured by an NADH molecule. This reaction is followed by eight different reactions occurring in the mitochondrial matrix, except for the sixth reaction catalyzed by succinate dehydrogenase, which takes place in the mitochondrial inner membrane. Also, energy is captured by $FADH_2$ in this step. At the end of eight reactions, one molecule of ATP, three molecules of NADH and one molecule of $FADH_2$ are produced from a single pyruvate molecule.

The last step of the cellular respiration is oxidative phosphorylation (OXPHOS), which comprises the electron transfer chain (ETC). This step occurs in the mitochondrial inner membrane and major part of the ATP is produced within this step of mitochondrial respiration (46). Briefly, ETC consists of five complexes involving NADH-dehydrogenase (complex I), succinate dehydrogenase (complex II), ubiquinone bc_1, (complex III), cytochrome c and cytochrome c oxidase (complex IV) and ATP synthase (complex V) (16). ETC reactions begin with the transfer of electrons from NADH and $FADH_2$, produced in glycolysis and Krebs cycle, to the complex I and end with the production of ATP and H_2O. Several complex-specific inhibitors are used for the investigation of the activity of these complexes. During the transport of electrons through the ETC complexes, protons are pumped into the mitochondrial inner membrane to generate the mitochondrial membrane potential (MMP or $\Delta\Psi m$) (62). Rotenone, antimycin A and oligomycin are used for the inhibition of complex I, complex III and complex V, respectively. Similarly, FCCP

or CCCP is used as an uncoupler to inhibit the ATP production by demolishing the proton gradient needed (77).

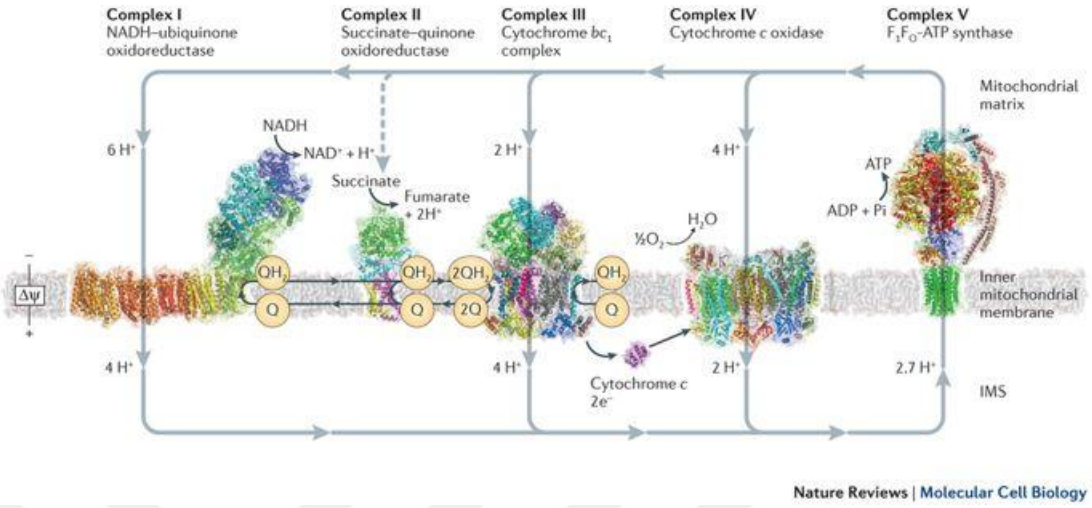

Figure 7. The electron transport chain. (89)

A small portion of electrons leak from the ETC, especially from complex I,II, and III and are transferred to oxygen in an unusual manner, and form superoxides (O_2^-). Superoxides formed within the complex I and II are released in to the mitochondrial matrix, whereas the ones formed in the complex III are released both into the intermembrane space and matrix (92). Mitochondrial ROS production is compensated by the transformation of the superoxides to hydrogen peroxide (H_2O_2) by superoxide dismutases (SOD). Low levels of ROS are beneficial for the cellular signalling and function. But high levels of ROS induce oxidative stress because of inadequate antioxidant capacity (78).

1.4.2. Mitochondrial dynamics

Mitochondria are highly dynamic compartments of the cell since they move along the cytoskeleton and show different morphologies depending on the environmental conditions. These two important characteristics of mitochondria compose the term ‘mitochondrial dynamics’ which refers to the mitochondrial fusion and fission events (91). Fusion of two adjacent mitochondria to exchange metabolites, enzymes and mitochondrial gene products results in the formation of a

single mitochondrion (90). On the other hand, mitochondrial fission involves the division of a single mitochondrion into two daughter organelles, an event which is essential to populate the dividing cells with adequate numbers of mitochondria (122). A delicate balance between fusion and fission is required for proper mitochondrial function. Any disturbance in this balance results in morphological changes (107).

Mitochondrial fusion is formed by two separate events: Fusion of mitochondrial outer membrane (MOM) and fusion of mitochondrial inner membrane (MIM). Different proteins such as Mitofusin 1 and 2 (MFN1 and MFN2) located in the outer membrane of mitochondria and Optic atrophy 1 (OPA1) situated in the inner membrane are responsible for these events (16).

Mitochondrial fission comprises of the recruitment of dynamin-related protein-1 (Drp1) from the cytosol to the mitochondrial outer membrane. Two important adaptor proteins, situated on the outer membrane play a role in this recruitment: Fission-1 (Fis1) and mitochondria fission factor (Mff) (90).

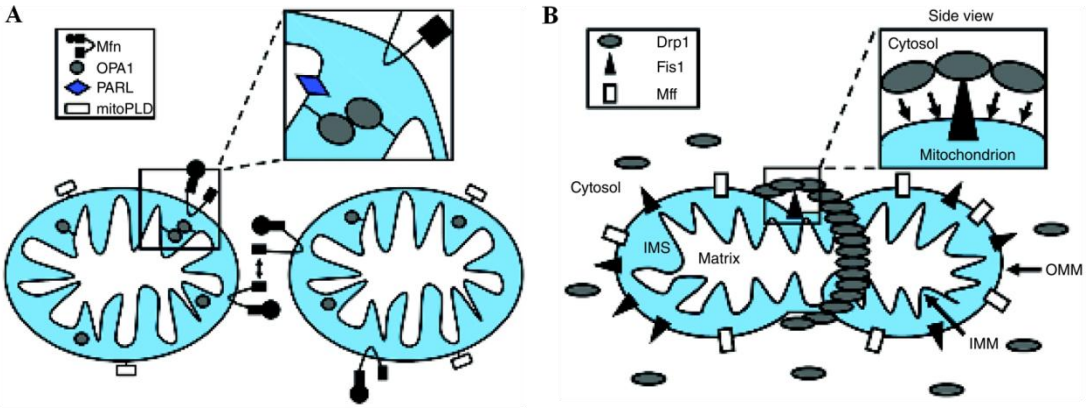

Figure 8. Representative images of mitochondrial fusion (A) and fission (B). (90)

1.4.3. Mitophagy

There exists several cellular mechanisms for the repair of damaged mitochondria including UPS, fusion and fission. Failure or inadequacy of these repair mechanisms enhance mitochondrial degradation. The key system for mitochondrial turnover is autophagic degradation of mitochondria, specifically named as mitophagy. Mitophagy can be induced by several stresses, such as oxidative damage, loss of mitochondrial membrane potential and hypoxia (85). Mitophagy mechanism is mediated by the receptors containing LC3-interacting region (LIR). LC3-II can recognize these regions, so that the damaged mitochondria can be engulfed in the autophagosome (65). The receptors mediating mitophagy are divided into three groups. The first group comprises the receptors located on the mitochondrial outer membrane, such as BNIP3, FUND1 and AMBRA1. The second group consists of cytosolic proteins like p62, NDP52, TAX1BP1, OPTN and NBR1. The most known mechanism mediated by cytosolic proteins is PINK1/Parkin mediated mitophagy. Briefly, in the case of mitochondrial membrane potential loss, PTEN-induced putative kinase 1 (PINK1) is accumulated on the mitochondrial outer membrane and phosphorylates ubiquitines (P-UB) to recruit Parkin. PINK1 activates Parkin by phosphorylation and triggers the phosphorylation of other proteins on mitochondrial outer membrane. At the end, damaged mitochondria are abundant in P-UB and this creates the ‘eat-me signal’ (52, 65). The last group of receptors includes cardiolipin, which is situated on the mitochondrial inner membrane under normal conditions. In the case of damaged mitochondria, cardiolipin is transported to the mitochondrial outer membrane and interacts with LC3-II to induce the ‘eat-me signal’ (85).

1.5. Neurodegeneration and Mitochondria

Proper neuronal function is highly dependent on mitochondrial metabolism, since these organelles are the main source of their high energy requirements. Exceptional morphology of neurons also makes them dependent on proper mitochondrial function, especially their axonal transport, to satisfy energy demands at neurite sites. Moreover, mitochondrial quality control mechanisms need to work adequately, because neurons are unable to diminish any damage by cell division as a consequence of their post-mitotic state. Any alterations in these mitochondrial

dynamics and quality control mechanisms would result in mutations in mtDNA, breakdown of mitochondrial integrity and network, decreased OXPHOS, inadequate ATP production and increased oxidative stress, which eventually make neurons vulnerable to degeneration (37). Hence, disturbed mitochondrial dynamics, along with the accumulation of misfolded or aggregated proteins, are among the common features of neurodegenerative diseases, including AD, PD and HD (65). However, it is still not clear whether mitochondrial dysfunction occurs because of aggregated proteins or conversely it promotes protein aggregation (85, 91).

1.5.1. Alzheimer's disease and mitochondria

Recent studies indicate that there is a strong relationship between mitochondrial dysfunction and early onset AD symptoms. Specifically, decreased glucose uptake was found in AD patients, followed by reduced enzyme activity, ATP production, decreased mitochondrial membrane potential and increased ROS formation (52). The compromised mitochondrial function can be related with three different conditions. First condition originates from the imbalance between mitochondrial fission and fusion dynamics and mitophagy. As described before, fusion and fission events occur to maintain a healthy mitochondrial network, morphology and to improve mitochondrial biogenesis. However, in the case of AD, the balance between these two events is disrupted in favour of fission, which results in fragmented morphology and reduced mitochondrial mass in AD brains. This aspect is proved by increased levels of Fis1 and Drp1; as the major proteins involved in fission; and decreased levels of Mfn1, Mfn2 and Opa1; as contributors of fusion; in AD brains and in *in vivo* models of AD (17). Together with this imbalance, impaired mitophagy is suggested to be effective in the pathogenesis of AD, since impaired autophagy is shown to play a role in AD. But the underlying mechanisms concerning the role of mitophagy in AD need further study (65).

The second compromised condition observed in AD is associated with mitochondrial energetics, manifested as reduced ATP production, change in Ca^{2+} metabolism and, most importantly, increased oxidative stress induced with abnormal

ROS production. Mitochondrial dysfunction can be correlated with Aβ and tau pathology, however they together form a vicious cycle such that they both can trigger one another. Therefore, the origins of the symptoms seen in AD remain controversial. Nevertheless, it is found that oxidative stress, as a consequence of excessive ROS production, trigger proteinopathies related with AD in the early onset of the disease (105). Besides, increased ROS production causes impairments in enzymatic activities involved in mitochondrial energy metabolism, like pyruvate dehydrogenase enzyme complex, and in ETC reactions involved in ATP production. Therefore, it induces the loss of mitochondrial membrane potential, mtDNA damage, leakage of mitochondrial contents into the cytosol and triggers neuronal death (58).

The third and the last condition seen in AD is impaired axonal transport of mitochondria. This situation can be associated with disrupted intracellular Ca^{2+} concentrations caused by increased ROS production and with microtubule dissociation due to hyperphosphorylated tau accumulation. Both are responsible from neurotransmission and synaptic function (23).

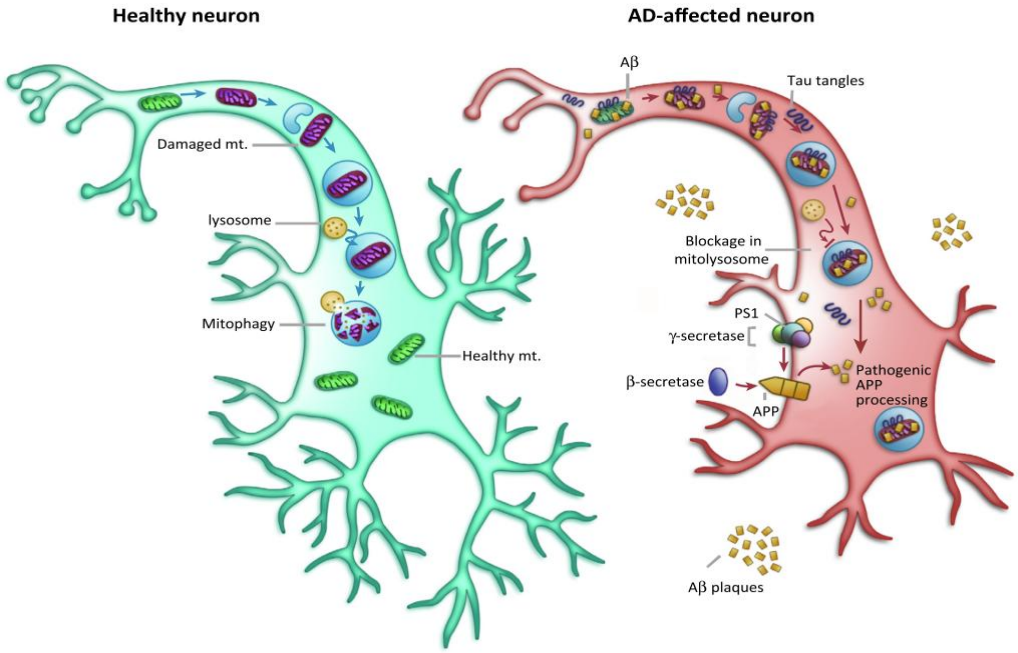

Figure 9. Mitochondrial dysfunction in AD. (52)

2. MATERIALS AND METHODS

2.1. Materials

Table 1. Reagents and resources list

Antibodies	
Alexa Fluor 488-conjugated goat anti-rabbit IgG (H+L)	ThermoFisher Scientific
Mouse monoclonal anti-beta Actin loading control (BA3R)	ThermoFisher Scientific
Mouse monoclonal anti-Neurofilament 70kDa (clone DA2)	Merck
Rabbit polyclonal anti-BECN1(H-300)	Santa Cruz
Rabbit polyclonal anti-LC3B	Sigma Aldrich
Rabbit monoclonal anti-Mitofusin-2 (D2D10)	Cell Signaling Technology
Rabbit polyclonal anti-p62/SQSTM1	Novus Biologicals
Peroxidase affinipure goat anti-mouse IgG (H+L)	Jackson Immunoresearch
Peroxidase affinipure goat anti-rabbit IgG (H+L)	Jackson Immunoresearch
Dyes	
DAPI	Sigma Aldrich
MitoSOX Red Mitochondrial Superoxide Indicator	ThermoFisher Scientific
MitoTracker Green FM	ThermoFisher Scientific
MitoTracker Red CMXRos	ThermoFisher Scientific
Thioflavin-T	Sigma Aldrich
Kits	
Cell Proliferation Kit I (MTT)	Roche
Cytotoxicity Detection Kit Plus (LDH)	Roche
Seahorse XFp Cell Mito Stress Kit	Agilent Technologies
Chemicals	
0% Fat Skim milk	Regilait
2-mercaptoethanol	Sigma Aldrich
3-Methyladenine (3-MA)	Sigma Aldrich
30% Acrylamide/Bis-acrylamide	Sigma Aldrich
$A\beta_{1-42}$ rat	Sigma Aldrich
Acetic acid	Sigma Aldrich
Amersham Hybond P 0.2 PVDF membrane	GE Healthcare
Amersham Protran 0.2 NC membrane	GE Healthcare
Ammonium persulphate	Sigma Aldrich
Bafilomycin A1 from streptomyces griseus	Sigma Aldrich
Bovine Serum Albumin (BSA) Fraction V	Roche
CDP-Choline	Fluka
Collagen IV from human placenta	Sigma Aldrich
cOmplete EDTA-free protease inhibitor cocktail	Roche
Color prestained protein standard, broad range	New England Biolabs
Dimethyl sulphoxide (DMSO) Hybri-Max	Sigma Aldrich
DTT	Applichem

Ethanol	Sigma Aldrich
Ethylenediaminetetraacedic acid (EDTA)	Sigma Aldrich
F-12 Nut Mix (Ham) 1X	Gibco
Glycerol	Sigma Aldrich
Glycine	Merck
Glucose monohydrate	Sigma Aldrich
HI Fetal Bovine Serum (FBS)	Gibco
HI Horse Serum (HS)	Gibco
Hydrochloric acid	Sigma Aldrich
Igepal CA-630	Sigma Aldrich
Methanol	Sigma Aldrich
Mounting medium	Ibidi
Nerve Growth Factor	Sigma Aldrich
Paraformaldehyde	Sigma Aldrich
Penicilin-Streptomycin	Gibco
Phenylmethanesulfonyl (PMSF)	Applichem
Phosphate Buffer Saline (PBS) (1X)	Gibco
Ponceau S	Sigma Aldrich
Potassium chloride	Sigma Aldrich
Potassium dihydrogen phosphate	Sigma Aldrich
Quick Start Bradford 1X Reagent	BioRad
Rapamycin from streptomyces	Sigma Aldrich
SDS	Sigma Aldrich
Sodium azide	Sigma Aldrich
Sodium chloride	Sigma Aldrich
Sodium fluoride	Sigma Aldrich
Sodium hydroxide	Merck
Sodium phosphate dibasic dodecahydrate	Sigma Aldrich
Sodium orthovanadate	Sigma Aldrich
Sodium Pyruvate 100mM (100X)	Gibco
SuperSignal West Pico Chemiluminescent Substrate	ThermoFisher Scientific
TEMED	Sigma Aldrich
Triton X-100	Sigma Aldrich
Trizma Base	Sigma Aldrich
Trypan Blue Solution	Sigma Aldrich
Tryple Select (1X)	Gibco
Tween-20	Sigma Aldrich
Western blotting filter paper	ThermoFisher Scientific

Equipment

4°C fridge	Kirsch
-20°C freezer	Kirsch
-80°C freezer	GLF
Biosafety cabinet	ThermoFisher Scientific
ChemiDoc MP Imaging System	BioRad
Cell culture incubator	
Confocal Microscope, LSM 700	Zeiss

Environmental shaker/incubator	ESCO
Flow cytometer, FACSVerse	BD
Micro centrifuge	ThermoFisher Scientific
Mini centrifuge	Biosan
Plate reader	BioTek
Seahorse XFp analyzer	Agilent Technologies
Trans-blot turbo transfer system	BioRad
Varioskan flash	ThermoFisher Scientific
Ventilated micro centrifuge	ThermoFisher Scientific

2.1.1. Preparation of chemicals for cell culture

Nerve Growth Factor (NGF) (100ng/µl)

25µg NGF containing vial was dissolved in 250µl PBS containing 1% FBS. 10µl aliquots were taken from 100ng/µl stocks and stored at -80°C.

CDP-Choline (10mM)

0.055g CDP-Choline was dissolved in 10ml sterile ddH_20 to prepare 10mM stocks. Filter sterilization was followed using 0.22µm filter. 200µl aliquots were taken and stored at -80°C.

Rapamycin (1mM)

1mg vial was dissolved in 1.094 ml DMSO to obtain 1mM main stocks. 20µl aliquots were strored at -20°C. 1µM working stock was freshly prepared with low serum medium. 200nM rapamycin treatment was applied for 1h at 37°C.

Bafilomycin A_1 (160µM)

2µg vial was dissolved in 20µl DMSO to prepared 160µM stock. 5µl aliquots were taken and stored in -80°C. 100nM working stock was freshly prepared with low serum before treatment. 5nM treatment was performed for 2h at 37°C.

3-MA (20mM)

2.25mg 3-MA was dissolved freshly in 1.5ml low-serum medium to prepare 20mM working stock. 5mM 3-MA treatment was followed at 37°C for 1h after filter sterilization step using 0.22µm filter.

$A\beta_{1-42}$

1mg vial was dissolved in 1ml sterile ddH_2O to obtain 226mM stocks. 15µl aliquots were taken and stored at -80°C. An aliquot was incubated at 37°C shaker for 2 days before use. Serial dilution steps in low-serum medium were performed for 12.5µM $A\beta_{1-42}$ treatment.

2.1.2. Gels, buffers and solutions

15% Acrylamide Gel (5ml)

30% Acrylamide/Bis-acrylamide	2.5ml
1.5M Tris (pH:8.8)	1.25ml
50% Glycerol	375µl
ddH_2O	875µl
10% APS	50µl
TEMED	5µl

12% Acrylamide Gel (5ml)

30% Acrylamide/Bis-acrylamide	2 ml
1.5M Tris (pH:8.8)	1.25ml
50% Glycerol	375µl
ddH_2O	1.375ml
10% APS	50µl
TEMED	5µl

4% Stacking (2.5ml)

30% Acrylamide/Bis-acrylamide	325µl
1 M Tris (pH:6.8)	625µl
20% SDS	12.5µl
ddH_2O	1.512ml
10% APS	12.5µl
TEMED	2.5µl

10X Tris-Glycine running buffer (pH 7.4-8.5)

0.25M Tris

1.92M Glycine

1% SDS

10X running buffer is diluted to 1X with ddH_2O

1X Transfer buffer

80% 1X Tris-Glycine running buffer

20% methanol

10X PBS (pH 7.4)

1.37M NaCl

0.03M KCl

0.035M KH_2PO4

0.1M $Na_2HPO_4.12H_2O$

10X PBS is diluted to 1X with ddH_2O

1X PBST

1X PBS

%0.5 Tween-20

1X RIPA lysis buffer

50mM Tris-HCl (pH 7.4)

150mM NaCl

1mM EDTA

1mM NaF

1mM Na_3VO_4

0.5% Igepal CA-630

0.5% Triton X-100

0.5mM PMSF in EtOH

1mM DTT

5X Loading Dye

250mM Tris-HCl (pH 6.8)

43.5% Glycerol

5% SDS

0.5% Bromophenol Blue

Ponceau S

0.1% (w/v) Ponceau S

5% Acetic acid

5% Skimmed Milk

5% (w/v) skimmed milk prepared in 1X PBST

5% BSA for primary antibodies

5% (w/v) Fraction V BSA

0.02% Na-Azide

Protease Inhibitor (PI)

1 tablet of Roche cOmplete EDTA-free protease inhibitor cocktail was dissolved in 2ml sterile ddH_2O to obtain 25X stock. 50µl aliquots were taken and stored at -20°C. Dilution to 1X was made with RIPA lysis buffer just before preparing cell lysates.

4% PFA for immunofluorescence

20g paraformaldehyde was dissolved in 500ml 1X PBS. pH of the solution was set to 7.2 with NaOH. Filter sterilization step was done using 0.22µm filter, 10ml aliquotes were taken and stored at -80°C.

Permeabilization buffer

0.2% Triton X-100 and 0.5% FBS containing PBS was filter sterilized using 0.2µm filter

Blocking buffer

PBS containing 0.1%Triton X-100, 0.5% FBS and 2mg/ml BSA was filtered with 0.2µm filter.

Washing buffer

0.1% Triton X-100 containing PBS was filtered through 0.2µm filter.

Antibody dilution buffer

0.1% Triton X-100, 0.5% BSA and 2mg/ml BSA containing PBS was filter sterilized using 0.2µm filter.

2.2. Methods

2.2.1. Cell culture

PC12-Adh cells (CRL1721.1, ATCC) were cultured in F12-Ham, containing 1% penicilin-streptomycin, 2,5% fetal bovine serum and 15% horse serum. Cells were maintained in a humidified atmosphere of 5% CO_2 at 37°C. Medium was changed every two days. Cells were splitted at 80% confluency. In all experiments, cells were seeded in complete medium. One day after seeding, cells were induced to differentiate with 30ng/ml NGF in low serum medium, which was F12-Ham medium, containing 1% penicilin-streptomycin and 1% horse serum, for five days. NGF containing LS medium was renewed every three days.

2.2.2. Determination of cell proliferation

PC12 cells were seeded at $2.5x10^4$ density in 96-well plates. 30ng/ml NGF differentiation was initiated for five days the day after seeding. Cells were incubated with increasing concentrations of $A\beta_{1-42}$ (1.25µM, 12.5µM, 50µM and 100µM) for 24 hours. Protocol of Cell Proliferation Kit I (MTT), Roche was followed to determine the effect of $A\beta_{1-42}$ on cell proliferation.

2.2.3. Determination of cytotoxicity

PC12 cells were seeded at $2.5x10^4$ density in 96-well plates. One day after seeding, 30ng/ml NGF incubation was performed for five days. Cells were incubated with increasing concentrations of $A\beta_{1-42}$ (1.25µM, 12.5µM, 50µM and 100µM) for 24h. Protocol of Cytotoxicity Detection Kit, Roche, was followed to determine the cytotoxic effects of $A\beta_{1-42}$.

2.2.4. Formation of $A\beta_{1-42}$ fibrils

226mM $A\beta_{1-42}$ stock was incubated at 37°C shaker for two days. Thioflavin-T binding assay was applied to investigate the formation of the fibrillar form of $A\beta_{1-}$42. For this purpose, blank mixture, composed of 10µM Thioflavin-T, 10mM Tris (pH 6.8), ddH_2O, and assay mixture composed of 10µM Thioflavin-T, 10mM Tris (pH 6.8) and 10µM $A\beta_{1-42}$, ddH2O were prepared. 60µl of each mixtures were put into 384-well black microplates in triplicates. Since Thioflavin-T gives emmision at 482nm in the presence of Aβ fibrils, fluorescence scan between 465nm and 600nm was followed using Thermo Varioskan instrument. Mean values were calculated from the triplicates.

2.2.5. Protein extraction

PC12 cells were seeded at $3x10^5$ density in 6-well plates. The day after seeding, 30ng/ml NGF incubation was initiated for five days. Cells were incubated with 100µM CDP-Choline for 48hours. 200nM rapamycin and 5nM bafilomycin treatments were followed for 1hour and 2 hours respectively. 12.5µM $A\beta_{1-42}$ injury was applied for 24 hours. Cell pellets were collected from each sample and lysed with appropriate amount of 1X RIPA lysis buffer and incubated on ice for 10min. After pipetting gently, another incubation on ice for 10 min was done. Afterwards, cells were centrifuged at 13000 rpm at 4°C for 10min. Supernatants were collected into new tubes and protein samples were stored at -20°C.

2.2.6. Protein concentration determination

After protein extraction, protein concentrations are determined by Bradford assay. For this purpose, 1.5, 0.75, 0.5, 0.25 and 0.125 µg/µl BSA standards are prepared. Protein samples are diluted in ddH_2O at 1:10 ratio and 10µl of each samples and BSA standards are put into a 96-well plate in triplicates. ddH_2o is used as blank. 190µl of 1X Bradford reagent is added onto each well and samples are incubated at dark for 5min at room temperature. After 5min, plate is read at 595nm. Mean values of each sample and BSA standards are calculated. Protein concentrations are calculated according to the equation obtained from BSA standard values.

2.2.7. SDS-PAGE and western blotting

5X loading dye was diluted to 1X with 15µg protein sample and heated at 95°C for 5min. Samples were loaded onto 15% and 12% acrylamide gels and run at 90V until all the samples reach to the bottom of the gel. Afterwards, gels were transferred to nitrocellulose or 0.2µm PVDF membrane by trans-blot semi dry blotting instrument for 25-30 min using 1X transfer buffer. To check whether the transfer was successful or not, membranes were stained with Ponceau S. Blocking step was followed using 5% skimmed milk solution prepared in PBST for 1h at room temperature. After blocking, membranes were probed with rabbit anti-LC3B (1:4000), rabbit anti-BECN1 (1:2000), rabbit anti-p62 (1:2000), mouse anti-neurofilament (1:1000), rabbit anti-mitufusin-2 (1:2000), mouse anti-β-actin (1:2000) primary antibodies overnight at 4°C. After washing membranes three times for 10min with PBST at room temperature, incubation with peroxidase-conjugated anti-mouse (1:2000) and anti-rabbit (1:2000) were followed for 1h at room temperature. Membranes were washed three times for 10min with PBST and SuperSignal West Pico chemiluminescent solution was applied onto membranes. Images were taken with ChemiDoc and analyzed with ImageLab program.

2.2.8. Immunofluorescence staining

13mm coverglasses were placed into 12-well plates and coated with 50ng/ml collagen from rat tail for 1h at 37°C. PC12 cells were seeded at $7x10^4$ density coverglasses in complete medium. Differentiation was initiated with 30ng/ml NGF

the day after seeding for 5 days. 100µM CDP-Choline, 200nM rapamycin, 5nM bafilomycin and 12.5µM $A\beta_{1-42}$ treatments were followed in the same way as in protein sample preparation. After treatments, cells were fixed with 4% PFA for 30 min at room temperature and washed with PBS. Permeabilization step was followed using permeabilization buffer for 20 min at room temperature, after this step samples were washed three times with washing buffer. Blocking buffer was applied for 15min at room temperature and samples were probed with rabbit anti-LC3B (1:500) using antibody dilution buffer at +4°C overnight. After washing three times with washing buffer, AF 488-conjugated anti-rabbit (1:1000) secondary antibody prepared in antibody dilution buffer was applied for 1h at room temperature. Samples were washed three times with washing buffer and two times with PBS, afterwards DAPI (1:5000) was applied for 15min at room temperature for nucleus staining. Samples were washed three times with PBS and coverglasses were mounted onto microscope slides. Images were taken with 63X oil objective using Zeiss LSM 700 confocal microscope.

2.2.9. Evaluation of mitochondrial dynamics with flow cytometry

PC12 cells were seeded at 10^6 density to 10cm cell culture dishes in complete medium. NGF-differentiation was initiated the day after seeding in low serum medium for five days. After differentiation, PC12 cells were incubated with 100µM CDP-Choline for 24 h, afterwards 12.5µM $A\beta_{1-42}$ treatment was followed for another 24h. After these treatments, cells were harvested and centrifuged at 600g for 5min. Pellets were dissolved in PBS and $2x10^5$ cells from each group were incubated with 50nM MitoTracker Red CMXRos, 2.5µM MitoSox and 200nM MitoTracker Green FM for 20min at 37°C to determine mitochondrial membrane potential, mitochondrial superoxide formation and mitochondrial mass respectively. Afterwards, samples were centrifuged at 600g for 5min and washed with PBS. Another centrifugation step was followed and pellets were dissolved in 200µl PBS. Samples were transferred to flow cytometry tubes and analyzed with BD FACS Verse flow cytometry instrument.

2.2.10. Mitochondrial staining

13mm coverglasses were placed into 12-well plates and coated with 50ng/ml collagen from rat tail for 1h at 37°C. PC12 cells were seeded at $7x10^4$ density coverglasses in complete medium. Differentiation was initiated with 30ng/ml NGF the day after seeding for 5 days. 100µM CDP-Choline treatment was followed for 24h after NGF differentiation. Afterwards, 12.5µM $A\beta_{1-42}$ treatment was initiated for 24h. After treatments, cells were washed with PBS and stained with 25nM MitoTracker Red CMXRos and 50nM MitoTracker Green FM for 15min at room temperature. After washing samples two times with PBS, coverglasses were mounted onto microscope slides and images were taken with 63X oil objective using Zeiss LSM 700 confocal microscope.

2.2.11. Measurement of mitochondrial respiration

A day prior this experiment, a Seahorse XFp Sensor Cartridge was hydrated using Seahorse XF Calibrant overnight at 37°C in a non-CO_2 incubator. Cells used for flow cytometry were processed for this experiment. Harvested and centrifuged PC12 cells were dissolved in PBS. $4x10^4$ cells from each group were seeded into Seahorse XFp Cell Culture miniplates in triplicates. These plates contain 8 wells, therefore only two experimental groups could be analyzed in one assay since two wells were considered as blank according to the manufacturers protocol. Plates were centrifuged at 300g for 1min without break, supernatant was discarded and 180µl XF Base Medium (pH 7.4), containing 1mM sodium pyruvate, 2mM L-glutamine, 10mM glucose, was added into wells. Cells were incubated in non-CO_2 incubator at 37°C for 40 min. During this incubation, the contents of Seahorse XFp Cell Mito Stress kit, which are oligomycin (50µM), FCCP (50µM), rotenone/antimycin A (25µM), were prepared according to manufacturers protocol. Afterwards, XFp Cell Mito Stress kit was applied as on the kit protocol and analyzed using Seahorse XFp analyzer.

2.2.12. Statistical analysis

Student's t-test was used for statistical analysis.

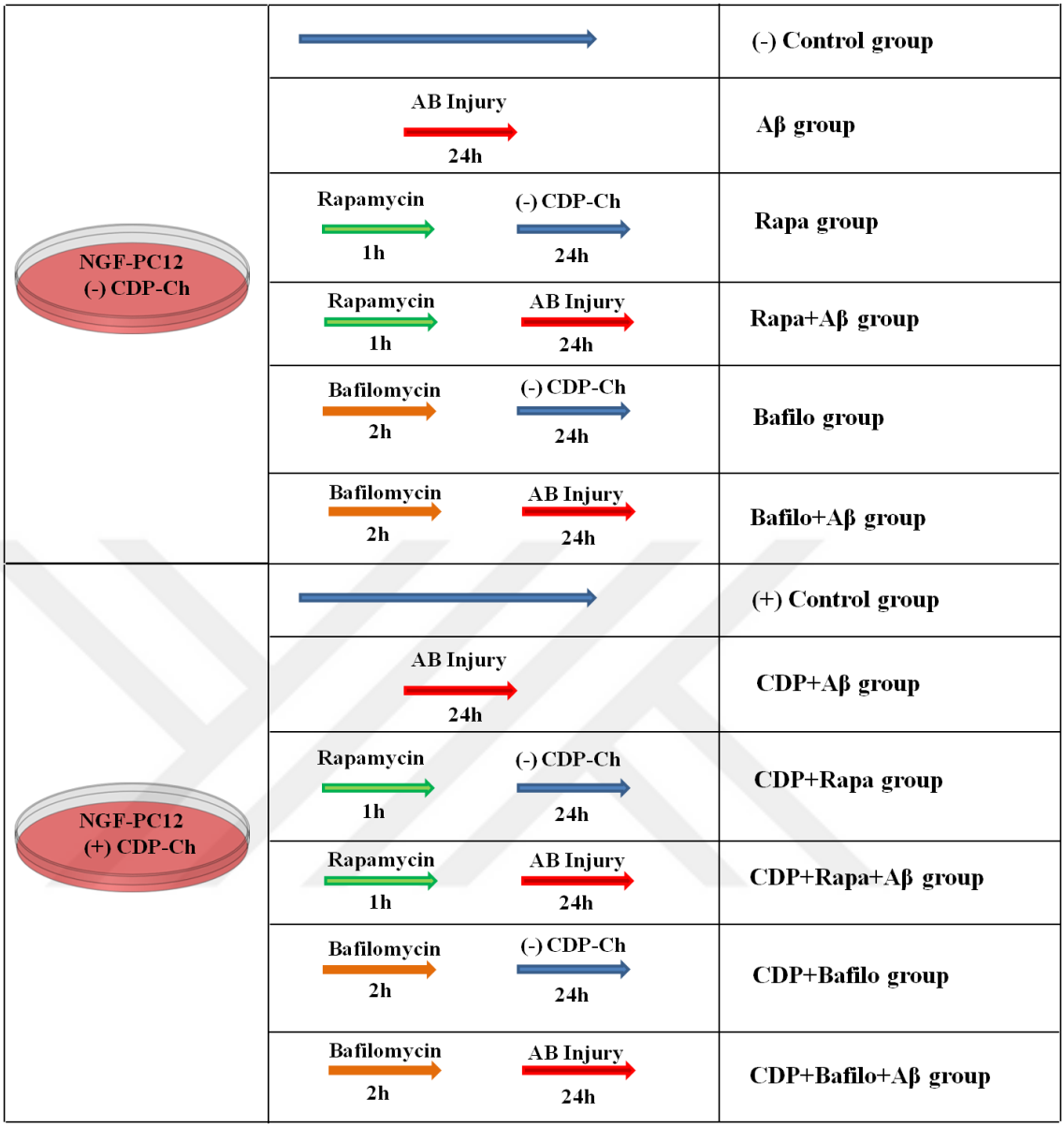

Figure 10. Experimental design

3. RESULTS

3.1. Effects of CDP-Choline on Autophagy Proteins in NGF-Differentiated PC12 Cells Upon $A\beta_{1-42}$ Injury

3.1.1. Differentiation of PC12 cells with Nerve Growth Factor (NGF)

NGF-differentiated PC12 cells are used as neuronal cell models. To determine the optimum duration for neuronal differentiation, PC12 cells were incubated with 30ng/ml NGF from three to six days. Cell morphologies were daily followed and images were taken under the light microscope for the observation of neurite growth. Neurite growth was detected at fifth day of NGF differentiation of PC12 cells compared to undifferentiated cells (Figure 11).

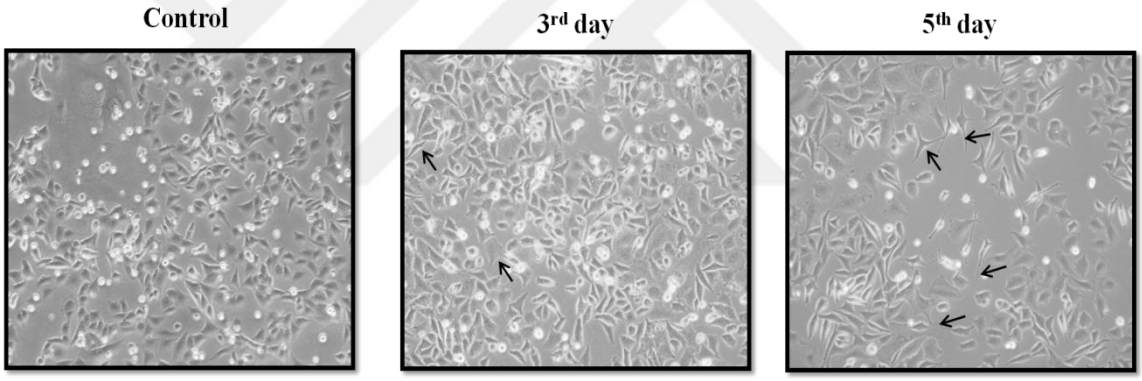

Figure 11. Neurite growth characterization of NGF-treated PC12 cells. PC12 cells were incubated with 30ng/ml NGF for three to six days. Morphological changes and neurite growth were analyzed daily, images were taken under a light microscope.

Differentiation of PC12 cells to neuronal cells in the presence of NGF can be characterized by several neuronal markers, such as neurofilament. There are several subunits of neurofilament, including neurofilament-L, neurofilament-M and neurofilament-H. In this work, we used neurofilament-L (~ 70kDa) for the determination of PC12 differentiation, since neurofilament-L forms heterodimers with other subunits. For this purpose, PC12 cells were incubated with 30ng/ml NGF three to six days. Samples were collected each day and neurofilament-70kDa levels were analyzed by western blotting. An increase in neurofilament levels was observed

on the fourth day of differentiation, compared to undifferentiated PC12 cells. Since the most distinct increase was seen on the fifth day, PC12 cells were differentiated with 30ng/ml NGF for five days in further experiments (Figure 12).

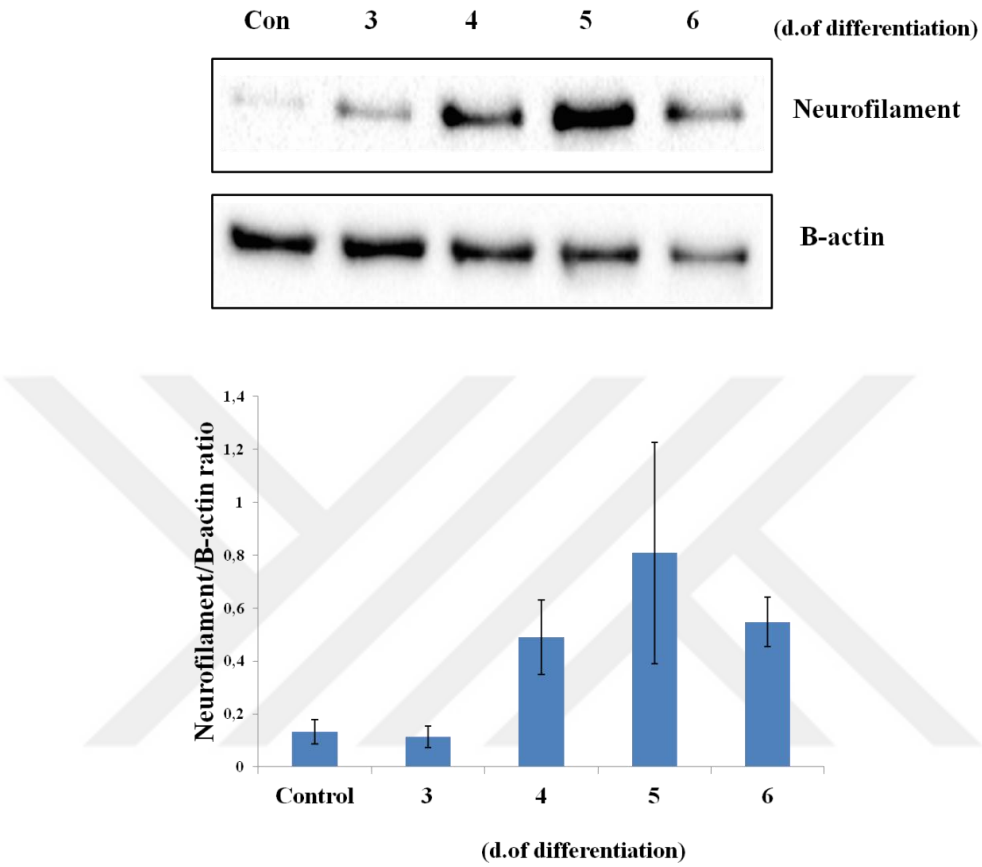

Figure 12. Neurofilament-70kDa levels of NGF-treated PC12 cells. PC12 cells were incubated in the presence of 30ng/ml NGF for three to six days. Samples were collected each day. Neurofilament-70kDa levels were analyzed with western blotting. Bar graph represents the mean ± values of three independent experiments.

3.1.2. Effect of CDP-Choline on autophagy proteins.

To study the effect of CDP-Choline on autophagy, differentiated PC12 cells were incubated in the presence and absence of CDP-Choline (100µM) up to 72 h. This concentration of CDP-Choline was chosen according to its effect on LCB levels in our preliminary work (data not shown). Samples were collected every 24 h and lysates were prepared to determine LC3B levels by western blotting. 16/18kDa ratio of LC3B was increased in both CDP-Choline treated and untreated cells for 48h (Figure 13). This increase was significant in the presence of CDP-Choline, p=0,03,

whereas it was not significant in the absence of CDP-Choline, p=0,24. Since the 16/18kDa ratio of LC3B increased at 48h of CDP-Choline treatment, we used this timepoint in further experiments.

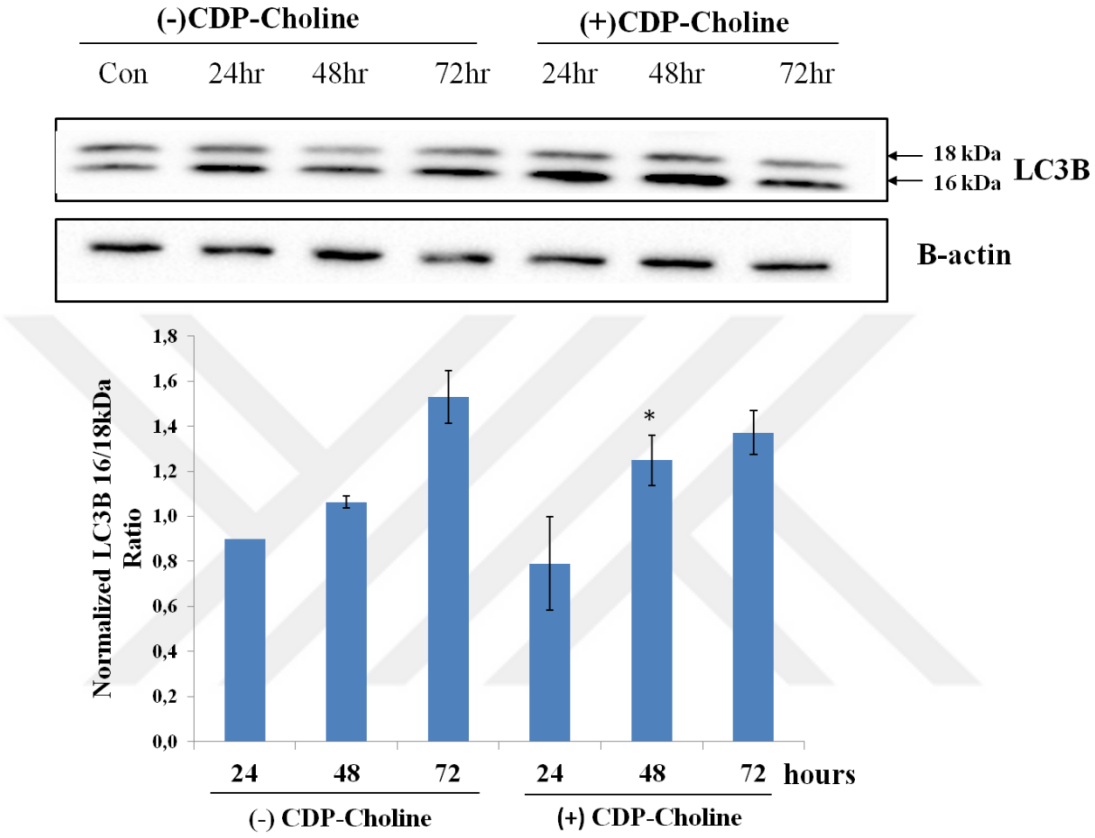

Figure 13. Effects of CDP-Choline on LC3B levels in differentiated PC12 cells. Differentiated PC12 cells were incubated in the presence and the absence of 100μM CDP-Choline up to 72h. Cell lysates were prepared every 24h. LC3B levels were studied by western blotting. Results are normalized to negative control group. Bar graph represents mean ± SEM values of three independent experiments.

To further analyze autophagy mechanism, p62 and BECN1 protein levels were also examined in the presence and the absence of CDP-Choline for 24-72 h in differentiated PC12 cells. CDP-Choline treatment did not significantly affect the protein levels of p62 and BECN1 as shown in Figure 14.

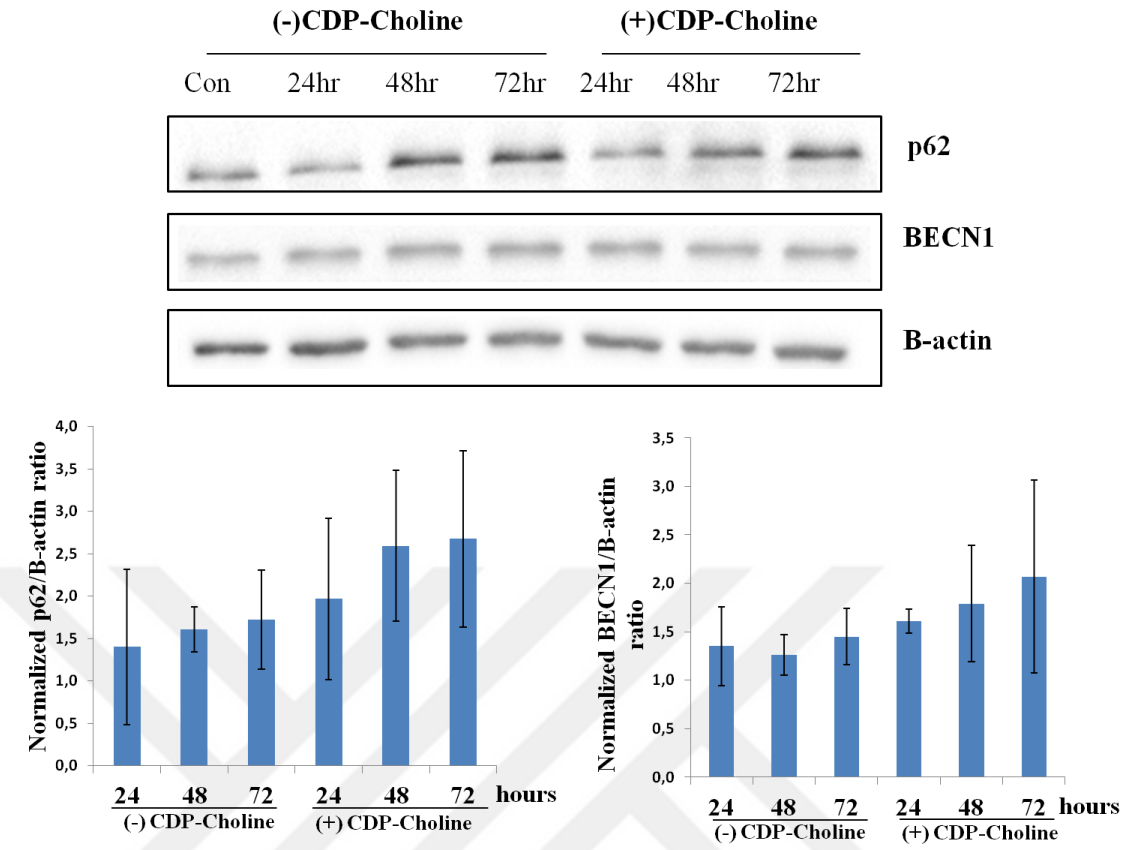

Figure 14. Effects of CDP-Choline on p62 and BECN1 levels in differentiated PC12 cells. Differentiated PC12 cells were cultured in the presence and the absence of 100µM CDP-Choline up to 72 h. Cell lysates were prepared every 24 h. p62 and BECN1 levels were measured by western blotting. Untreated cells were used as control and the results were normalized to the control group. Bar graphs represent the mean ±SEM values of three independent experiments.

3.1.3. Measurement of cytotoxicity of $A\beta_{1-42}$ on PC12 cells and its effects on cell proliferation.

To determine the cytotoxic effects of $A\beta_{1-42}$, NGF-differentiated PC12 cells were incubated with increasing concentrations of $A\beta_{1-42}$ (1.25µM, 12.5µM, 25µM, 50µM and 100µM) for 24 h. Cytotoxicity of $A\beta_{1-42}$ and its effects on cell proliferation were measured with LDH and MTT assays, respectively. According to these assays, $A\beta_{1-42}$ decreased cell proliferation in a concentration dependent manner. Particularly, a significant decrease was observed at 12.5µM, p=0.01, compared to the control group (Figure 15-A). Furthermore, $A\beta_{1-42}$ did not show a concentration-dependent change

in cytotoxicity. There was an increase until 50µM, but a slight decrease at 100µM. Besides, as seen on MTT assay, 12.5µM $A\beta_{1-42}$ caused a significant increase in the cytotoxicity of PC12 cells, p=0.03 (Figure 15-B). Therefore, this concentration was selected for use in further experiments.

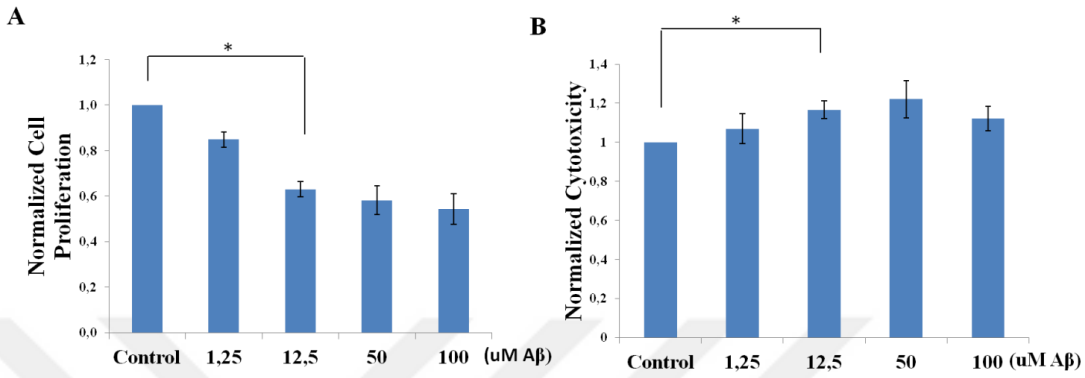

Figure 15. Cytotoxicity of $A\beta_{1-42}$ and its effects on cell proliferation. Differentiated PC12 cells were incubated with increasing concentrations of $A\beta_{1-42}$ for 24 h. MTT and LDH assays were performed to measure the effects of $A\beta_{1-42}$ on cell proliferation (A) and its cytotoxicity respectively (B). The untreated cells were used as control, and the results were normalized to the control group. Bar graphs respresent the mean ± SEM values of five independent experiments.

3.1.4. Measurement of fibrillar $A\beta_{1-42}$ formation.

Thioflavin-T, which is a fluorescent indicator of Aβ fibrils, was used to measure the fibrillar formation of $A\beta_{1-42}$. For this purpose, equal amounts of Thioflavin-T (10µM) were incubated with either $A\beta_{1-42}$ or 10mM of Tris (pH:6.8), which was the blank buffer solution. Fluorescence intensity of $A\beta_{1-42}$ was apparently increased between 465nm and 600nm, compared with the blank solution. This increase indicated the formation of fibrillar form of $A\beta_{1-42}$ (Figure 16).

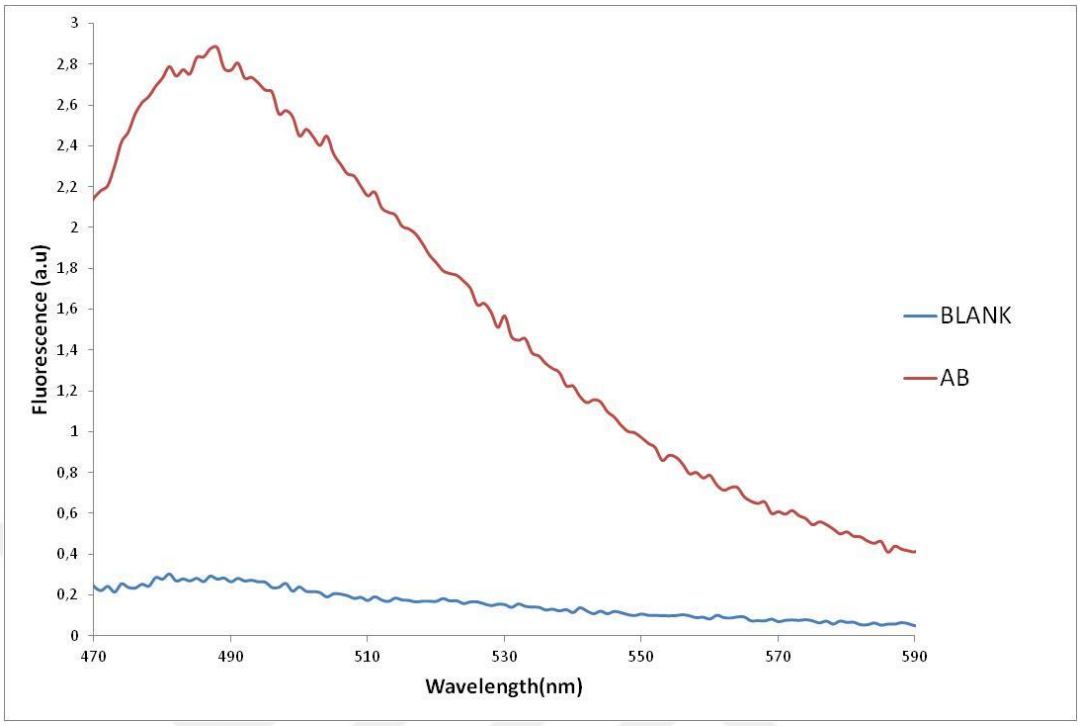

Figure 16. Thioflavin-T binding assay. 10µM of Thioflavin-T was incubated with either $A\beta_{1-42}$ or blank buffer solution. Fluorescence scanning between 465nm and 600nm results showed that there was an increase in the fluorescence intensity of $A\beta_{1-42}$ fibrils. The graph is representative of three independent experiments.

3.1.5. Determination of autophagy inducer and inhibitor concentrations.

Different autophagy inducers and inhibitors are used in literature to assess autophagic flux. We used rapamycin ,which is a mTOR inhibitor and widely used for the induction of autophagic activity to investigate the details of the effects of CDP-Choline and cell injury. To determine the optimum concentration of rapamycin, differentiated PC12 cells were cultured with increasing concentrations of rapamycin (0-200nM) for 1h. Samples were collected after 24 h and cell lysates were prepared to detect LC3B levels by western blotting. 200nM of rapamycin treatment increased 16/18kDa levels of LC3B compared to untreated PC12 cells. Therefore, 200nM rapamycin was used as autophagy activator in further experiments (Figure 17).

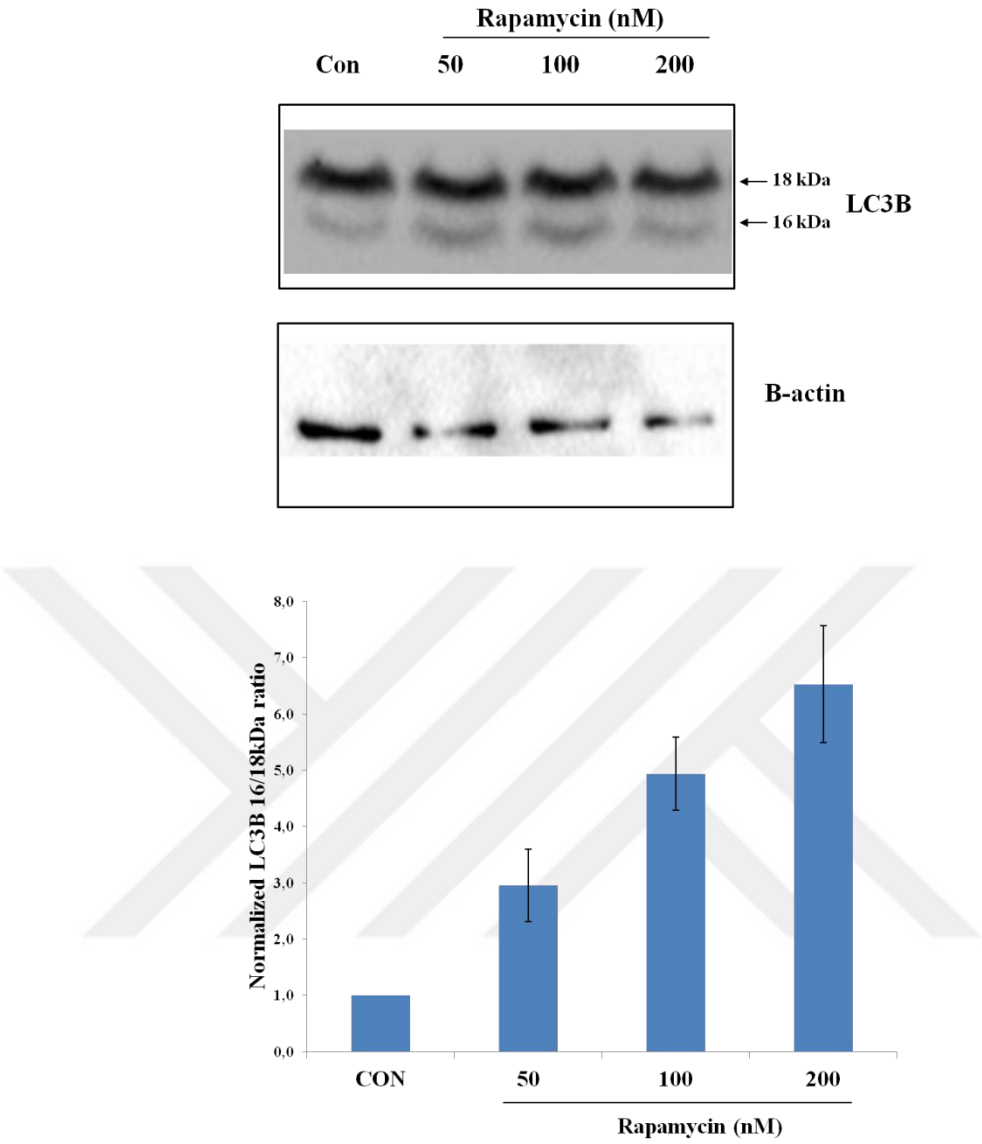

Figure 17. Determination of optimum rapamycin concentration. Differentiated PC12 cells were incubated with increasing concentrations of rapamycin (0-200nM) for 1 h. Samples were collected after 24 h. LC3B levels were analyzed by western blotting. Untreated cells were used as control and results were normalized to the control group. Bar graph represents mean ± SEM values of three independent experiments.

In order to measure autophagic flux in the presence of autophagy inhibitors, we used 3-MA, which is a blocker of class III PI3K inhibitor, involved in autophagosome formation, and bafilomycin, which acts as a V-ATPase inhibitor and blocks the lysosomal degradation of autophagosomal contents. NGF-differentiated PC12 cells were incubated with increasing concentrations of 3-MA (0-10mM) and bafilomycin (0-25nM) for 1 h and 2 h, respectively to determine optimum

concentrations of both inhibitors. Samples were collected after 24 h and LC3B levels were studied by western blotting. Although 3-MA causes a decrease in 16kDa/18kDa ratio of LC3B; we observed increased 16/18kDa ratio of LC3B in NGF-differentiated PC12 cells. This can be correlated with the effect of 3-MA on several pathways involving PI3K activity other than autophagy. On the other hand, bafilomycin showed an increase in 16/18kDa ratio, as expected. We also tested the effects of 5nM bafilomycin under same conditions on LC3B levels and observed and increase in 16/18kDa ratio (data not shown). In line with these results, we decided to use 5nM bafilomycin in further experiments as an autophagy inhibitor (Figure 18).

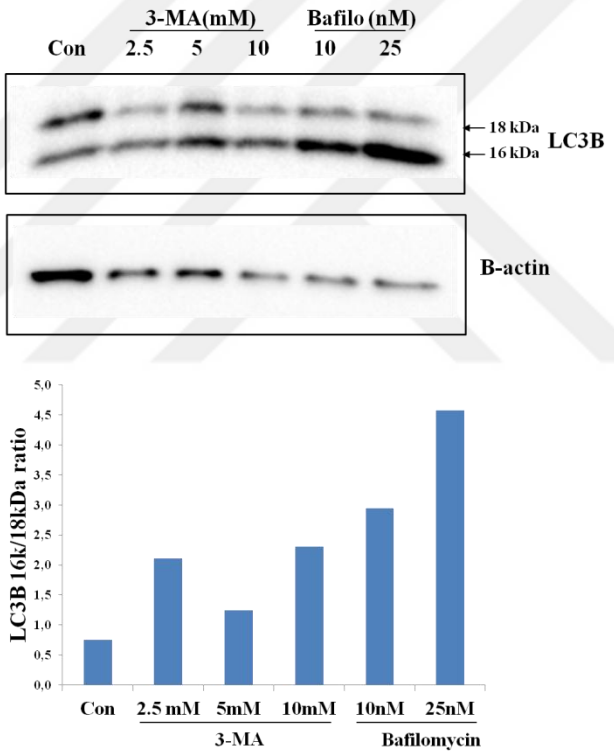

Figure 18. Determination of optimum inhibitor concentration. Differentiated PC12 cells were incubated with different concentrations of 3-MA (0-10mM) and bafilomycin (0-25nM) for 1h. and 2h. respectively. Samples were collected after 24h. and LC3B levels were analyzed by western blotting. Untreated cells were used as control.

3.1.6. Changes in the autophagy protein levels upon $A\beta_{1-42}$ injury.

Upon 100μM CDP-Choline treatment of NGF-differentiated PC12 cells for 48 h, cells were exposed to $A\beta_{1-42}$ injury for an additional 24 h. To clarify the role of CDP-Choline on autophagic flux, rapamycin and bafilomycin were used as autophagy inducer and inhibitor, respectively. LC3B levels of cell lysates were analyzed by western blotting. A significant increase in the 16/18kDa ratio of LC3B was observed in the presence of 100μM CDP-Choline, p=0.04. This result was consistent with the previous data (Figure 13). We also observed that this increase of LC3B caused by CDP-Choline was enhanced in the presence of rapamycin and bafilomycin. This indicated that 100μM CDP-Choline treatment cause an increase in autophagic flux. $A\beta_{1-42}$ injury also caused a significant increase in the 16k/18kDa ratio of LC3B, p=0.01. (Figure 19).

In addition to LC3B levels, we also investigated BECN1 levels, as another autophagy marker protein. Results suggested that there is an increase in BECN1 levels of CDP-Choline and $A\beta_{1-42}$ treated cells compared to the control group. Even though this increase was not statistically significant, p=0.23, p=0.14 respectively, it can be connected to the increase in LC3B levels (Figure 20).

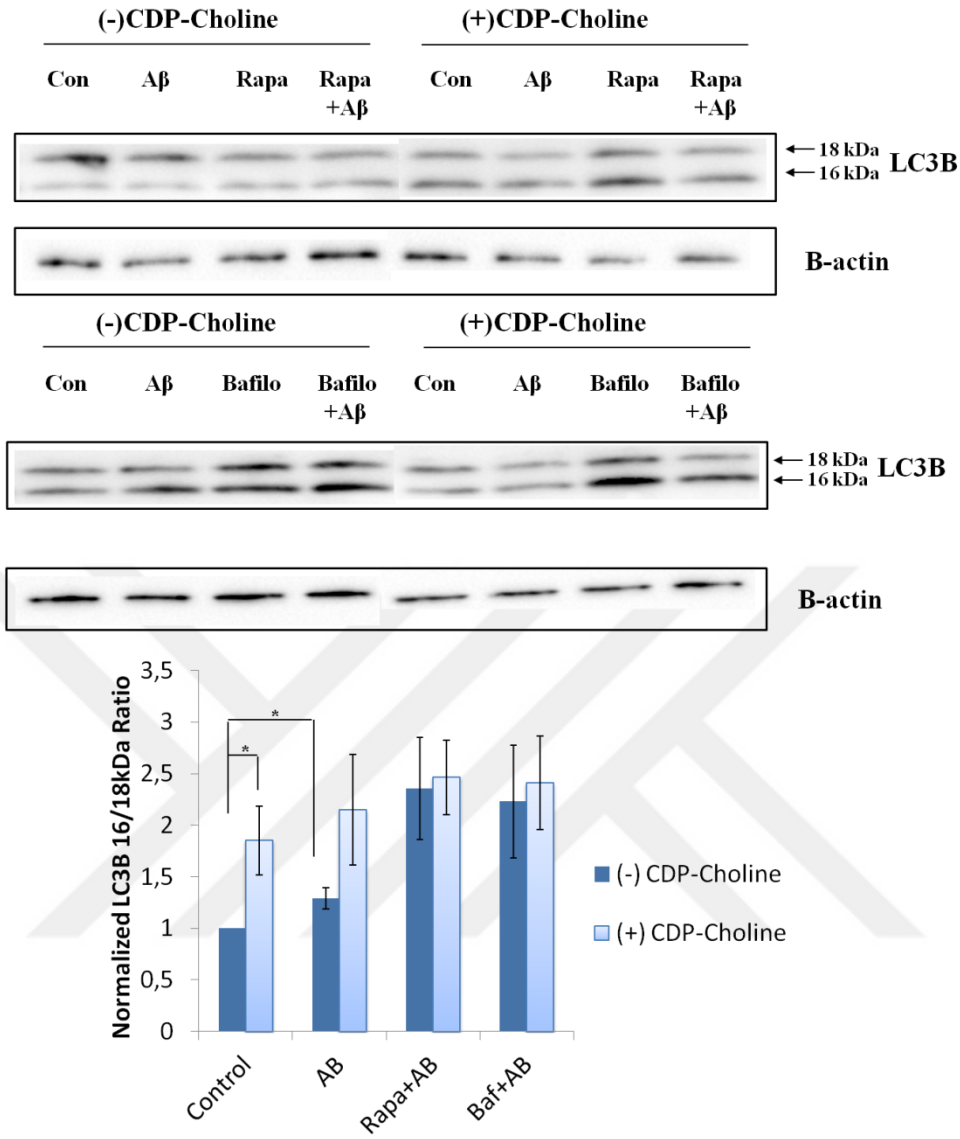

Figure 19. Effects of CDP-Choline on LC3B levels of injured PC12 cells. Differentiated PC12 cells were incubated in the presence and the absence of 100µM CDP-Choline for 48 h. $A\beta_{1-42}$ injury was followed for 24 h. Rapamycin and bafilomycin treatments were done in the presence and the absence of both CDP-Choline and $A\beta_{1-42}$. Cell lysates for each group were prepared for western blot analysis. LC3B results were normalized to negative control group. Bar graph represents mean ± SEM values of four independent experiments.

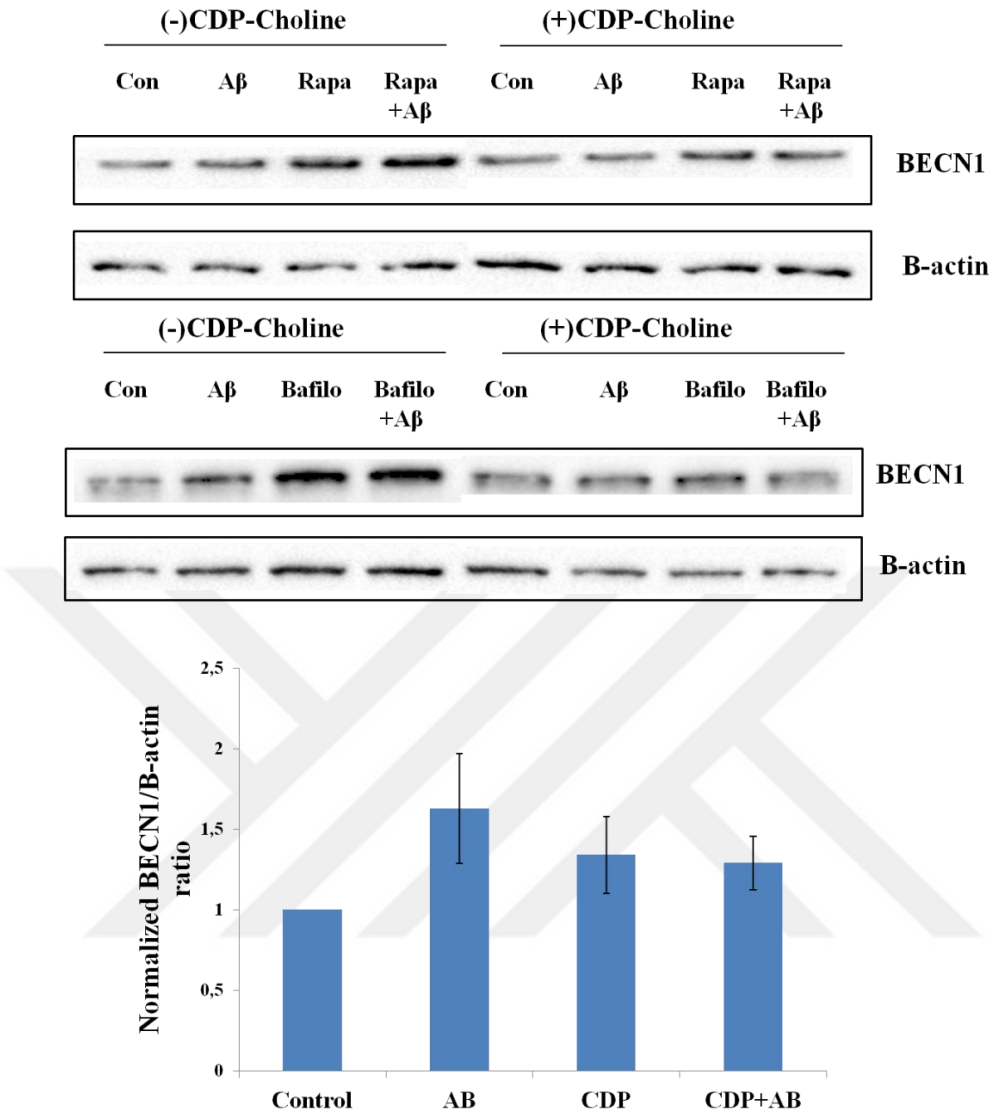

Figure 20. Effects of CDP-Choline on BECN1 levels of injured PC12 cells. Differentiated PC12 cells were incubated in the presence and the absence of 100µM CDP-Choline for 48 h. $A\beta_{1-42}$ injury was followed for 24 h. Rapamycin and bafilomycin treatments were done in the presence and the absence of both CDP-Choline and $A\beta_{1-42}$. Cell lysates for each group were prepared for western blot analysis. Results were normalized to negative control group. Bar graph represents mean ± SEM values of three independent experiments.

Immunofluorescence was followed concurrently with western blotting, and average LC3B puncta formation per cell was also analyzed. According to these results, average puncta per cell was significantly increased in the presence of 100µM CDP-Choline and 12.5µM $A\beta_{1-42}$, p=0.007 and p=0.02 respectively, which was consistent with our western blot results (Figure 21).

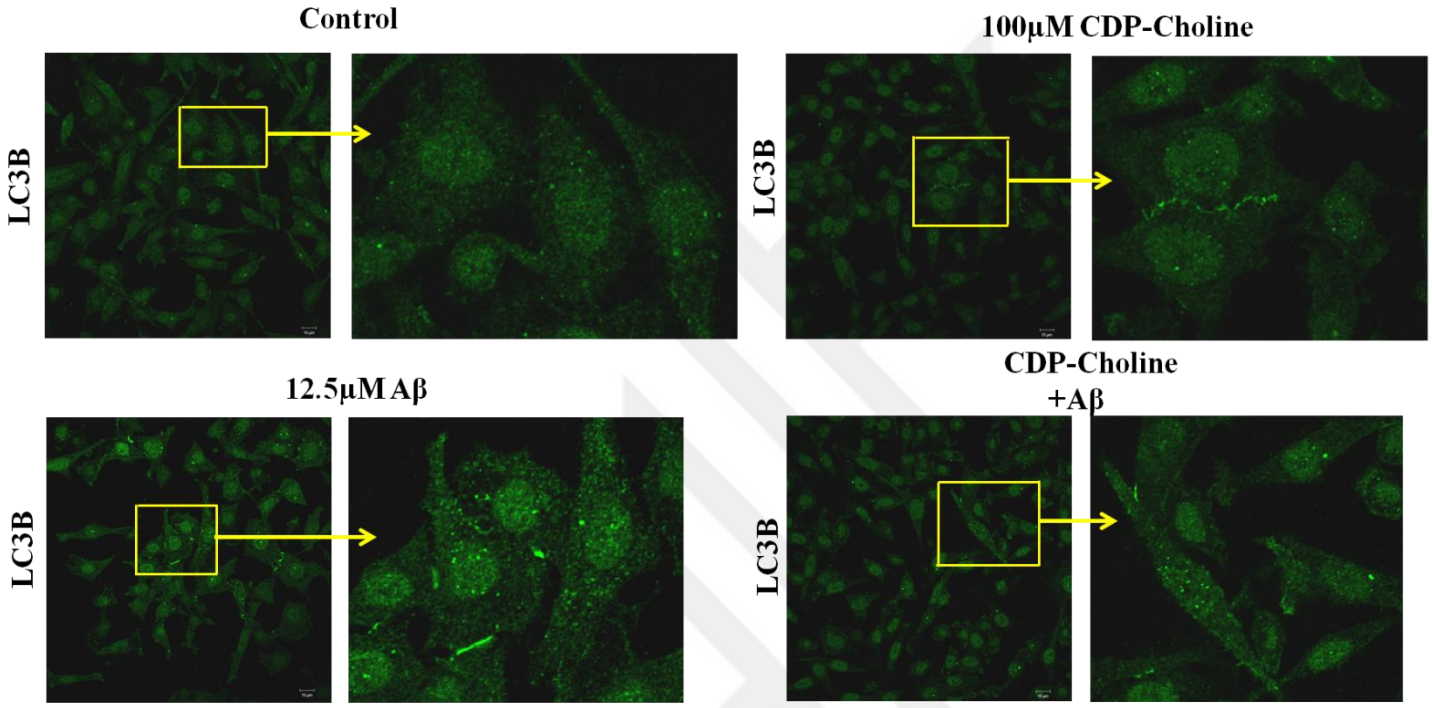

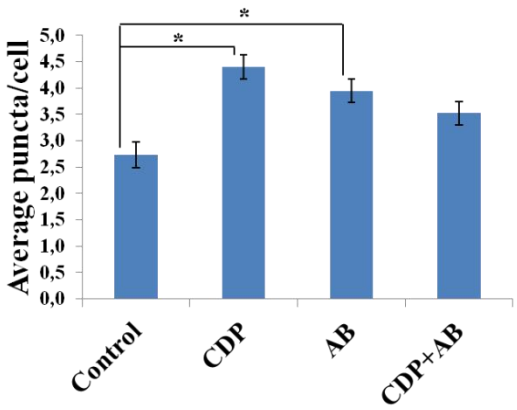

Figure 21. Observation of effects of CDP-Choline on injured PC12 cells with immunofluorescence.
Differentiated PC12 cells were incubated in presence and the absence of 100µM CDP-Choline for 48 h. $A\beta_{1-42}$ injury is followed for another 24h. Cells were fixed, probed with LC3B and stained with Alexa fluor 488- conjugated secondary antibody. DAPI was used for nucleus staining. Images were taken with 63X oil objective using Zeiss LSM 700 confocal microscope. Puncta formation per cell was counted for analysis. Images are representatives of three independent experimrnts, and the bar graph represents the mean ± SEM values of puncta formation.

3.2. Effects of CDP-Choline on Mitochondrial Dynamics of NGF-Differentiated PC12 Cells Upon $A\beta_{1-42}$ Injury

Mitochondrial dynamics constitute an important factor on mitochondrial, consequently cellular homeostasis and function. Mitochondrial dysfunction results in the development of various diseases, including neurodegenerative disorders. The effect of CDP-Choline on mitochondrial dynamics was studied to understand its potential neuroprotective role on $A\beta_{1-42}$ injured PC12 cells.

Mitofusin-2 is an important protein for mitochondria since it is the marker of mitochondrial fusion which is among the principal events in controlling mitochondrial dynamics. Therefore, we firstly investigated Mitofusin-2 levels of differentiated PC12 cells. Samples were prepared as described on section 3.1.6. Mitofusin-2 levels of the cell lysates were analyzed by western blotting. Even though the presence of CDP-Choline and $A\beta_{1-42}$ resulted in an increase of Mitofusin-2 levels, this was not statistically significant, $p=0.08$ and $p=0.07$ respectively. In addition, there was no difference between CDP-Choline treated and untreated cells upon $A\beta_{1-42}$ injury (Figure 22).

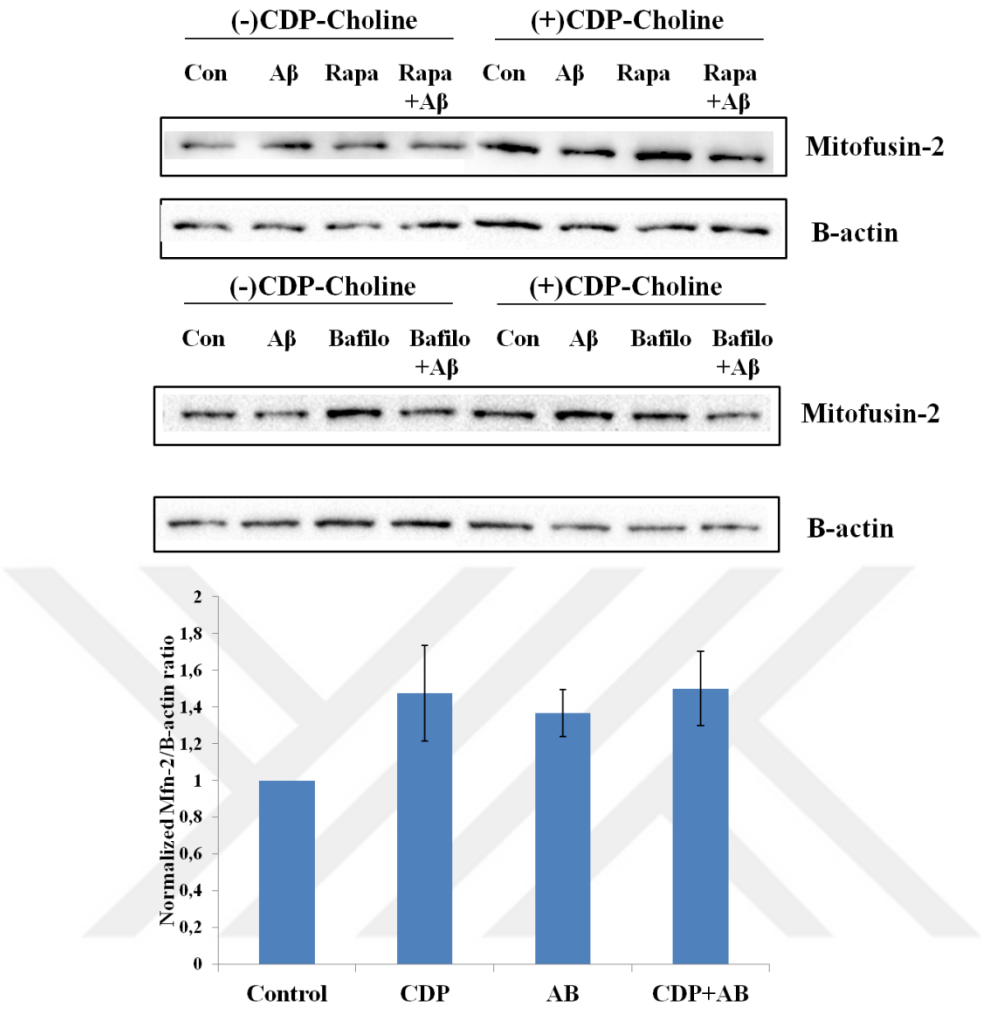

Figure 22. Effects of CDP-Choline on Mitofusin-2 levels of injured PC12 cells. Differentiated PC12 cells were incubated in the presence and the absence of 100µM CDP-Choline for 48 h. $A\beta_{1-42}$ injury is followed for 24 h. Rapamycin and bafilomycin treatments were done in the presence and the absence of both CDP-Choline and $A\beta_{1-42}$. Cell lysates for each group were prepared for western blot analysis. Results were normalized to negative control group. Bar graph represents mean ± SEM values of four independent experiments.

The effect of CDP-Choline on mitochondrial membrane potential was studied on differentiated PC12 cells. To this end, PC12 cells were incubated with increasing concentrations of CDP-Choline (100-1000µM) for 24 h. After incubation, cells were probed with MitoTracker Red CMXRos, which is sensitive to mitochondrial membrane potential. We did not observe any concentration dependent differences in mitochondrial membrane potential of PC12 cells between control and CDP-Choline (Figure 23-A). To identify the effect of CDP-Choline in a time-dependent manner,

differentiated PC12 cells were incubated with 100µM CDP-Choline for different timepoints (16h-72h) and probed with MitoTracker Red CMXRos. There was no change in mitochondrial membrane potential levels between control and CDP-Choline groups at different timepoints (Figure 23-B).

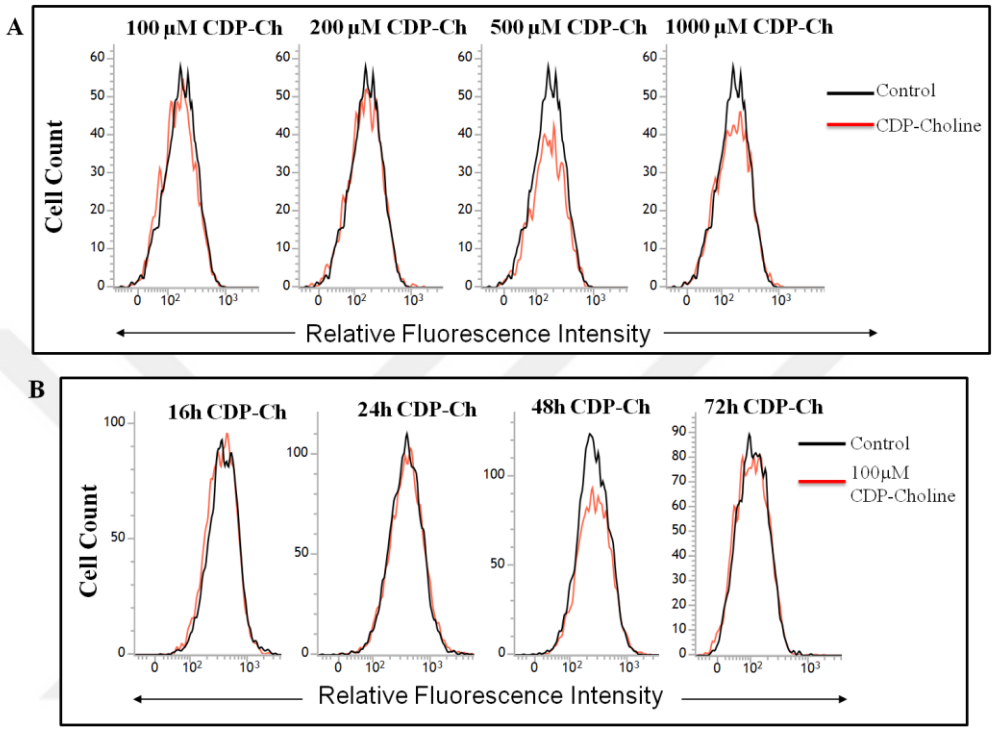

Figure 23. Effects of different concentrations of CDP-Choline on mitochondrial membrane potential. Differentiated PC12 cells were incubated with increasing CDP-Choline concentrations (100-1000µM) for different timepoints. After incubation, cells were probed with 50nM MitoTracker Red CMXRos, measured by flow cytometry and analyzed with BD FACS Suite program. (A) Incubation with increasing concentrations of CDP-Choline for 24 hours did not cause any change in mitochondrial membrane potential on PC12 cells. (B) Incubation with 100µM CDP-Choline for different timepoints did not change the mitochondrial membrane potential of PC12 cells.

Upon 100µM CDP-Choline treatment of differentiated PC12 cells for 24 h, 12.5µM $A\beta_{1-42}$ injury was followed for another 24 h. Cells were probed with MitoTracker Red CMXRos, MitoSox and MitoTracker Green FM to monitor mitochondrial membrane potential, mitochondrial superoxides and mitochondrial mass, respectively by flow cytometry. When $A\beta_{1-42}$ treated group was compared with control group, we observed a significant increase in MitoRed levels, p=0.03. Although there was an enhancement in the MitoSox levels in $A\beta_{1-42}$ treated group as well, it was not statistically significant, p=0.08. MitoGreen levels were also enhanced

in $A\beta_{1-42}$ treated group, but it was not a significant increase, p=0,15. When CDP-Choline treated group was compared with the control group, a significant increase was noticed in MitoSox levels, p=0.04. Interestingly, a significant increase was also observed in MitoGreen levels, p=0.03. We did not observe any changes in MitoRed levels of control group and CDP-Choline-treated group, which was consistent with our previous data (Figure 23). Additionally, we did not notice any change in MitoRed, MitoSox and MitoGreen levels when we compared Aβ treated group with CDP+Aβ treated group (Figure 24).

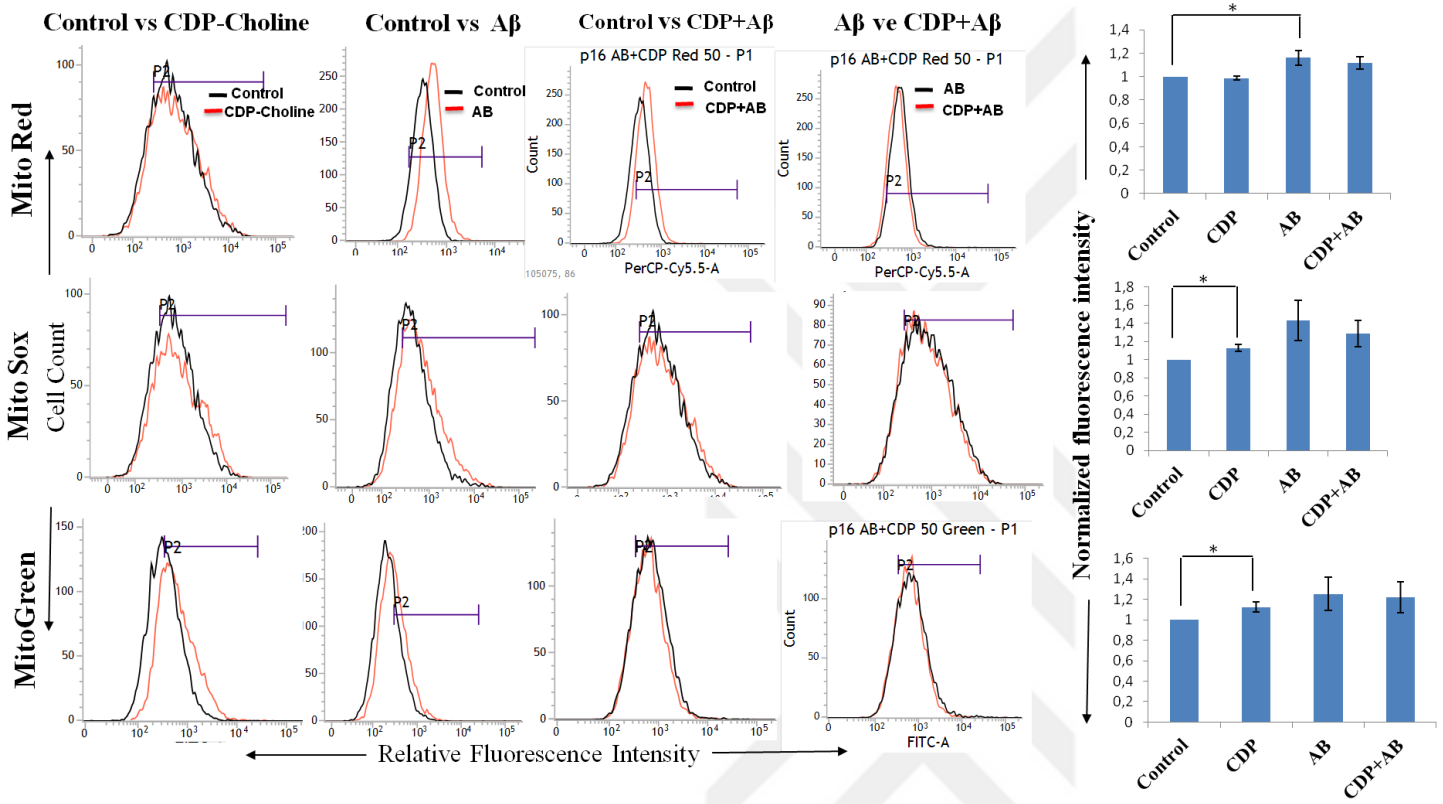

Figure 24. Analysis of the effects of CDP-Choline on mitochondrial dynamics with flow cytometry. Differentiated PC12 cells were cultured in the presence and the absence of 100µM CDP-Choline for 24 h. Afterwards, PC12 cells were exposed to 12.5µM $A\beta_{1-42}$ injury for another 24 h. Cells were probed with 50nM MitoTracker Red CMXRos, 2.5µM MitoSox and 200nM MitoTracker Green FM to study mitochondrial membrane potential, mitochondrial superoxides and mitochondrial mass respectively. Fluorescence intensity of the probed cells were obtained with flow cytometry and analyzed with BD FACS Suite program. Histograms are representatives of six independent experiments and show the relative fluorescence intensity of compared groups. Results were normalized to control group. Bar graphs represent mean ± SEM values of six independent experiments.

Confocal microscopy imaging was followed concurrently to verify the results obtained from flow cytometry. To this end, NGF-differentiated PC12 cells were treated as described in Figure 24 and were probed with MitoTracker Red CMXRos and MitoTracker Green FM. Consistent with our flow cytometry results, an increase was observed in MitoRed levels when control and $A\beta_{1-42}$ groups were compared. Similarly, a noticable enhancement was obtained in MitoGreen levels between control and CDP-Choline treated groups (Figure 25). Apart from these, we did not observe any notable changes in other groups.

In addition to flow cytometry analysis, mitochondrial respiration was examined simoultaneosly using *XFp Cell Mito Stress* kit of Seahorse XFp analyzer. $A\beta_{1-42}$ injury was followed for 24 h upon 100μM CDP-Choline treatment for 24 h. Samples were processed according to the manufacturers protocol for analysis. Oligomycin, FCCP and mixture of rotenone and antimycin A were used as ETC complex V inhibitor, uncoupler and ETC complex I and III inhibitor, respectively. According to these experiments, cells treated with 100μM CDP-Choline had decreased mitochondrial respiration rates with reference to the control group. Maximal respiration and ATP production rates of CDP-Choline treated group were also lower than the control group (Figure 26-A,C). Likewise, mitochondrial respiration, maximal respiration and ATP production decreased in cells treated with both CDP-Choline and $A\beta_{1-42}$ compared with only $A\beta_{1-42}$-treated group (Figure 26-B,D).

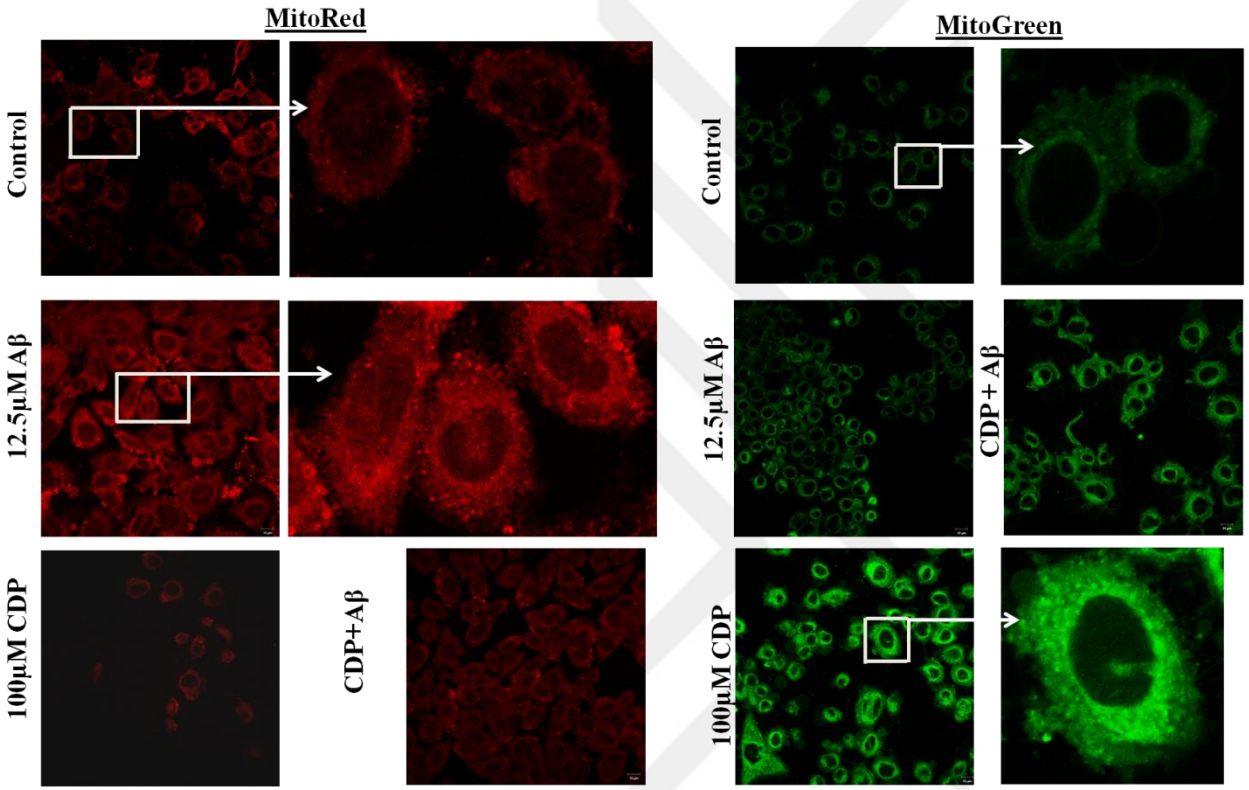

Figure 25. Analysis of the effects of CDP-Choline and $A\beta_{1-42}$ on mitochondrial dynamics with confocal microscopy. Differentiated PC12 cells were incubated in the presence and the absence of 100µM CDP-Choline for 24 h. Afterwards cells were treated with 12.5µM $A\beta_{1-42}$ for 24 h. Cells were probed with 25nM MitoTracker Red CMXRos and 50nM MitoTracker Green FM.Images were taken with 63X oil objective using Zeiss LSM 700 confocal microscope. Representative images were selected from three independent experiments.

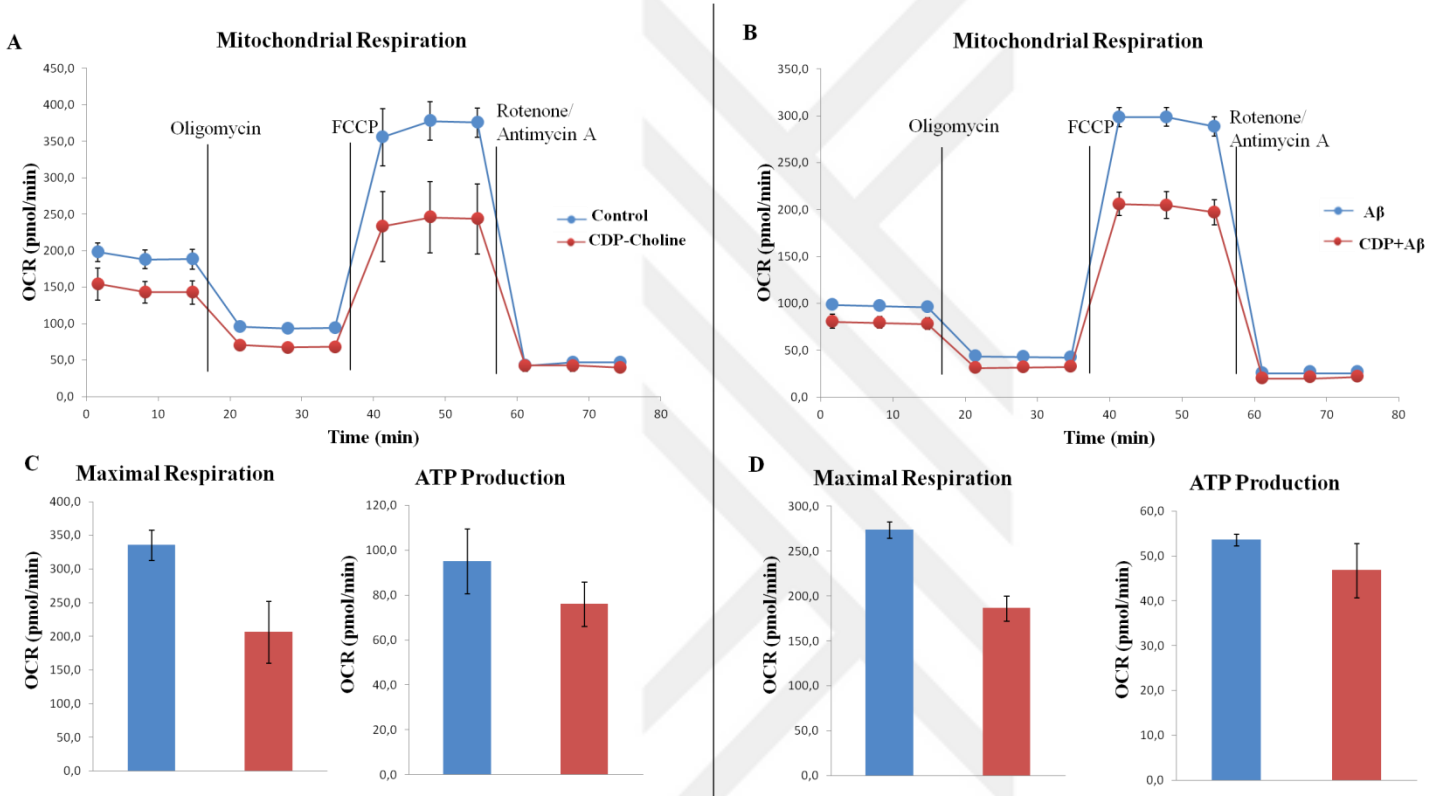

Figure 26. Analysis of mitochondrial respiration rates of CDP-Choline and $A\beta_{1-42}$ treated PC12 cells. Differentiated PC12 cells were cultured in the presence and the absence of 100µM CDP-Choline for 24 h. Afterwards, incubation with 12.5µM $A\beta_{1-42}$ was followed for 24 h. XFp Cell Mito Stress kit is used for the analysis of mitochondrial respiration using Seahorse XFp Analyzer. 1µM Oligomycin, 2µM FCCP and 500nM mixture of rotenone and antimycin A were used as ETC complex V inhibitor, uncoupler and ETC complex I and III inhibitors respectively. Graphs are representatives of three independent experiments and show mean ± SD values obtained by three consecutive readings of each sample at each step.

To evaluate the effect of higher concentrations of $A\beta_{1-42}$ on mitochondrial dynamics, NGF-differentiated PC12 cells were pre-treated with 100µM CDP-Choline for 24 h and then, incubated with 50µM $A\beta_{1-42}$ for another 24 h. Cells were probed with MitoTracker Red CMXRos, MitoSox and MitoTracker Green FM as previously described. Interestingly, CDP-Choline treatment decreased MitoSox levels in the presence of 50µM $A\beta_{1-42}$. Besides, we observed a decrease in MMP levels of Aβ-injured PC12 cells. However, CDP-Choline did not affect mitochondrial mass upon injury (Figure 27).

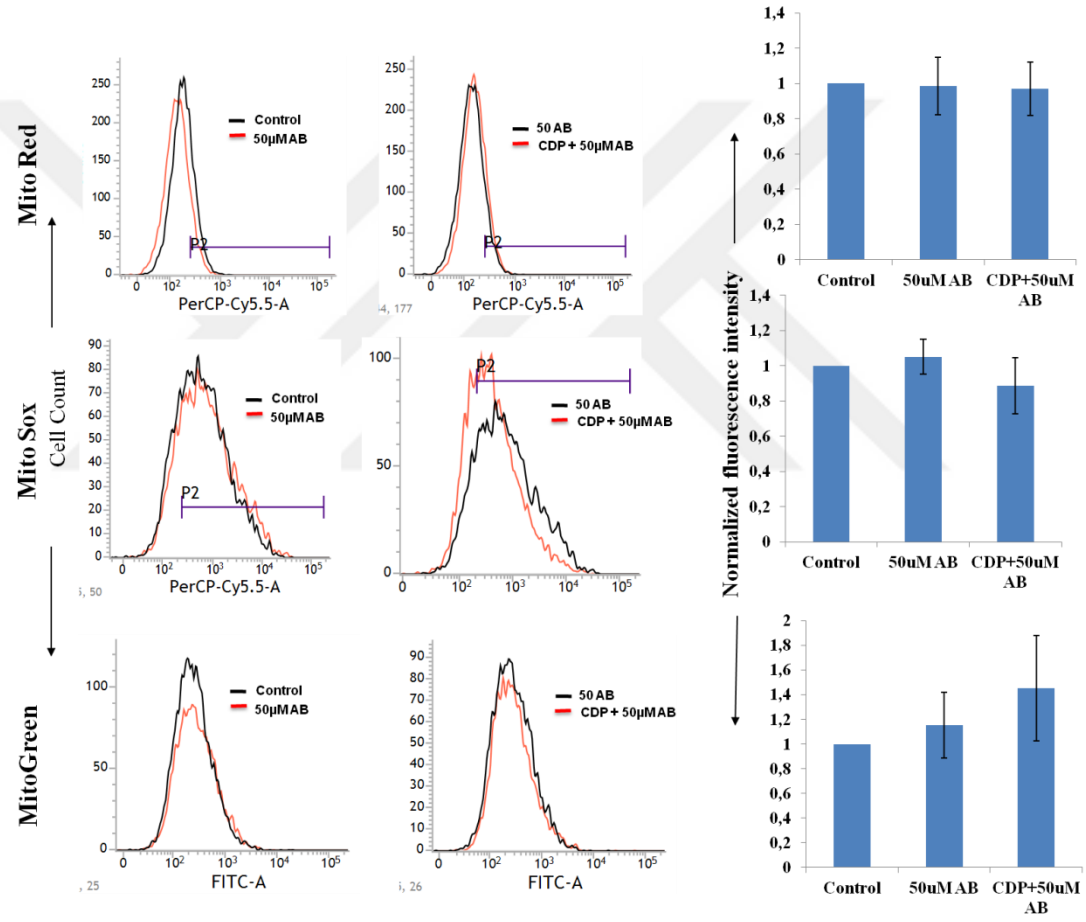

Figure 27. Effects of 50µM $A\beta_{1-42}$ treatment on mitochondrial dynamics of differentiated PC12 cells. Differentiated PC12 cells were treated with 100µM CDP-Choline for 24 h. 50µM $A\beta_{1-42}$ incubation is followed for another 24 h. Mitochondrial membrane potential, mitochondrial superoxides and mitochondrial mass are analyzed by probing cells with 50nM MitoTracker Red CMXRos, 2.5µM MitoSox and 200nM MitoTracker Green FM, respectively. Fluorescence intensity of the probed cells are obtained with flow cytometry and analyzed with BD FACS Suite program. Histograms are representatives of three independent experiments and show the relative fluorescence

intensity of compared groups. Fluorescence intensities are analysed using BD FACS Suite program. Results are normalized with control group. Bar graphs represent mean ± SEM values of three independent experiments.

4. DISCUSSION

AD is the most prevalent neurodegenerative disease worldwide by affecting over 44 million people and predicted to exceed 130 million people in 2050 due to increasing life expectancy. Treatment and medical expenses for this disease are also anticipitated to exceed a trillion-dollars in a few years. Currently used drugs for AD treatment are unable to stop or reverse the symptoms of the disease, therefore AD-related investigations are still the key to find an effective treatment. Formation of senile plaques composed of aggregated Aβ and hyperphoshorylated tau mediated NFTs are accepted as the major causes of AD. These effects result in neuronal degeneration and loss followed by cognitive deficits and memory loss. The mechanism underlying these pathologies remains elusive. Although, autophagy mechanism is considered as a potential therapeutic and protective pathway to clear aggregated and misfolded proteins seen in AD, enhancement in autophagic levels were also reported in neurodegeneration. Besides, accumulated AVs are reported to be a source of toxic Aβ peptides. Therefore, these situations render autophagy as a double-edged sword since its role still remains controversial. In addition, the membrane source of the autophagosome still remains unknown. Recent studies highlighted the neuroprotective effects of CDP-Choline, which is an intermediate in PC synthesis, in *in vivo* and *in vitro* models of brain hypoxia, ischaemia, intracerebral haemorrhage, and traumatic brain injury (36). However, the mechanism of this neuroprotective effect of CDP-Choline needs to be elucidated. PC, as the major constituent of biological membranes, also plays a role in maintaining neuronal homeostasis, including neurotransmission and synaptic function. Given the findings indicating reduced PC and PE levels in AD brains, CDP-Choline is suggested to be a precursor to ameliorate phospholipid synthesis (6, 75). In view of the involvement of autophagosome in autophagy mechanism, we proposed that CDP-Choline might enhance autophagic activity by providing lipid sources for autophagosome formation. Therefore, in this study we aimed to examine effects of CDP-Choline on autophagy in NGF-differentiated PC12 cells upon $A\beta_{1-42}$ injury.

Since the effect of CDP-Choline on autophagy of neuronal cells is unknown, we firstly characterized neuronal differentiation of PC12 cells following NGF treatment. We measured neurofilament-70kDa levels known as a neuronal marker during differentiation process. Neurite outgrowth was observed on the fifth day of differentiation. Next, the effect of CDP-Choline on autophagy proteins of differentiated PC12 cells were investigated. The levels of LC3B, the most important autophagy marker, were investigated. Statistically significant increase in 16/18kDa ratio of LC3B protein was detected following 48 h of CDP-Choline treatment of differentiated PC12 cells. In addition to LC3B levels, the other autophagy proteins, BECN1 and p62 were also followed upon CDP-Choline treatment. However, we did not determine a significant change in these protein levels as similar to that observed in LC3B levels. In a rat model of ischemia/reperfusion, protective effects of choline treatment via regulating autophagic flux have been recently reported (37). Autophagy induction upon CDP-Choline treatment on differentiated PC12 cells was demonstrated for the first time with our study. We did not observe any difference in BECN1 and p62 levels upon CDP-Choline treatment of differentiated PC12 cells. This may be a result of their roles in different cellular pathways other than autophagy, including redox homeostasis, inflammatory responses and endocytosis, aging and apoptosis respectively (4, 111). To this end, Wooten et al. (113) showed increased p62 levels in NGF-differentiated PC12 cells activates NF-κB pathway for cell survival. In addition, McNight et al. (66) demonstrated the involvement of Beclin-1 protein in membrane trafficking pathways, like endocytosis, and neuronal viability via UVRAG-Vps34 complex.

Different concentrations of Aβ have been used for inducing cell injury in other studies (28, 117). Therefore, we examined the effect of different $A\beta_{1-42}$ concentrations (1.25; 12,5; 50; 100μM) on cell proliferation and toxicity to determine optimum conditions for cell injury. We found that 12.5μM $A\beta_{1-42}$ treatment significantly increased cytoxicity and reduced cell viability by nearly 30%. To figure out the effects of CDP-Choline on autophagy in the presence and the absence of $A\beta_{1-42}$, LC3B protein levels were measured. A significant increase was

detected in 16/18kDa ratio of LC3B protein of the cells treated with $A\beta_{1-42}$. In addition to western blot experiments, immunofluorescence analysis of LC3B levels consistently revealed a significant increase in puncta formation per cell in Aβ and CDP-Choline treated PC12 cells. Similar effect of $A\beta_{25-35}$-mediated injury on LC3B levels was also shown by Pengjuan Xu et al. in 2015 (116). But they did not investigate the effects of Aβ injury on autophagic flux. Furthermore, enhanced 16/18kDa ratio of LC3B of Aβ treated cells in the presence of rapamycin and bafilomycin, as inducer and inhibitor of autophagy, showed that Aβ induces autophagic flux (70). Although the details about the mechanism of this induction need further investigation, Hung SY et al. (45) showed that induced autophagic flux protects SHSY-5Y cells from Aβ injury via a7-nicotinic-acetylcholine receptors (a7nAChR).

Since mitochondria are the main power suppliers for cellular events their proper function is necessary for cellular homeostasis. Mitochondrial fusion and fission events, and mitophagy are together responsible for mitochondrial quality control. These events are triggered by changes in mitochondrial membrane potential or disruption in bioenergetics involving mitochondrial respiration. As previously described, fusion and fission events are involved in the exchange of mitochondrial contents and division of damaged parts of the mitochondrion, respectively. On the other hand, mitophagy is involved in the autophagosomal engulfment of damaged mitochondria and their degradation upon fusion with lysosome. There is a substantial increase in the number of publications highlighting the importance of mitochondrial homeostasis via mitochondrial dynamics and mitophagy in neurodegenerative diseases. Although mitochondrial dysfunction and altered bioenergetics are among the indicators of AD, it is still not clear whether these indications are consequences or reasons of proteinopathies seen in AD. The effects of CDP-Choline on mitochondrial dynamics of differentiated PC12 cells in the presence and the absence of Aβ injury have been investigated in this thesis study for the first time. CDP-Choline treatment enhanced the levels of Mfn2, which are involved in mitochondrial fusion. This result is consistent with increased mitochondrial mass seen in our flow

cytometry analysis. Thus, CDP-Choline may have a role in preserving the delicate balance between mitochondrial dynamics and bioenergetics by enhancing fusion between healthy and damaged mitochondria. Mitochondrial dynamics are altered in AD brains in favor of mitochondrial fission, followed by fragmented mitochondrial morphology and decreased fusion protein levels (109). Interestingly, our results showed increased Mfn2 levels upon Aβ injury. This may reflect the differences between *in vitro* and *in vivo* models of AD. Due to their highly dynamic structures, mitochondria should undergo fusion and fission in short time periods to maintain homeostasis. Hence, assessing mitochondrial fusion after 24 h may be misleading since the essential effect of Aβ or CDP-Choline on mitochondrial dynamics can be captured at earlier timepoints.

MMP is a key element in mitochondrial function and fate, resulting from protons pumped into the mitochondrial inner membrane during electron transfer through ETC complexes in OXPHOS. MMP is considered to be an indicator of cellular ATP metabolism since it is responsible from the initiation of ATP synthesis. Besides, dissipation of MMP triggers mitophagy by recruiting and phosphorylating Parkin to the mitochondrial outer membrane, a process conceived as 'eat-me!' signal (85, 129). OXPHOS, as the fundamental mechanism for cellular ATP synthesis, is a naturally ROS producing system. Under normal conditions, mitochondrial ROS are produced following binding of leaked electrons to oxygen. ROS production can be handled and utilized in signalling pathways as long as it is balanced by antioxidant production induced by SOD and glutathione reductase activity. However, in the case of neurodegeneration, including AD, ROS are overproduced and cause increased oxidative damage resulting in neuronal loss. Increased mitochondrial ROS levels are related to several factors, including, decreased ATP production and changes in the protons pumped into the intermembrane space (59). Similarly, oxygen consumption and ATP production rates are also diminished with aging and neurodegenerative diseases. Recent studies indicate that CDP-Choline is effective in neuroprotection by increasing ATP production, acetylcholine production and glutathione reductase levels (53, 106). Similarly, its antioxidant effects have been shown in different

disease models (2, 35, 126). In this study, MMP, mitochondrial superoxide formation, mitochondrial mass and oxidative phosphorylation in cells treated with CDP-Choline and Aβ were analysed in order to clarify the role of CDP-Choline on mitochondrial function. Although CDP-Choline did not cause any alterations in MMP levels of NGF-differentiated PC12 cells, a significant increase in MitoSox levels was observed upon CDP-Choline treatment. Also, a decline in oxygen consumption rate was detected in CDP-Choline treated cells. These results, combined with increased Mfn2 levels and mitochondrial mass may be associated with impaired mitophagic activity, since inactivation of Mfn2 by phosphorylation mediated by PINK1 is required for the recruitment of Parkin to the mitochondrial outer membrane (17, 20). Furthermore, a study in 2015 demonstrated Mfn2 deficient MEF cells exhibited increased OCR levels (51). Similarly, increased MitoSOX levels can be associated with decreased OCR levels upon CDP-Choline treatment, since oxygen molecules become vulnerable to leaked electrons during OXPHOS. In addition, a recent study involving neuronal stem cells (NSCs) indicates increases in ROS levels and mitochondrial mass as an intermediate step in neurogenesis (9). Although we did not study the effect of CDP-Choline on neurogenesis, increased MitoSox levels and mitochondrial mass upon CDP-Choline treatment may be related with neurogenesis. In addition to these results, we found that 12.5μM Aβ treated PC12 cells showed interestingly a significant increase in MMP levels compared to the control group, whereas their MitoSOX and MitoGreen levels did not change. These results can be associated with altered bioenergetics and impaired mitophagy upon Aβ treatment. Diminished ATP synthesis is correlated with increased MMP (62), whereas mitophagy deficits are shown as a cause of increased MMP levels and mitochondrial protein accumulation, such as Mfn2 (44). Moreover, Sun L et al. (99) showed enhanced PINK1/Parkin mediated mitophagy in response to acetylcholine to attenuate injury caused by hypoxia in myoblast cells. Since CDP-Choline may be involved in acetylcholine production (114), it is possible that CDP-Choline treatment would enhance mitochondrial function by increasing acetylcholine levels to prevent neuronal loss. Although 12.5μM Aβ treatment caused an increase in cytotoxicity, it did not affect MitoSox and MitoRed levels as expected. Hence, it left question marks about the effectiveness of our AD model with aggregated Aβ peptides. We further

analyzed the effects of 50μM Aβ-mediated injury on mitochondrial dynamics of differentiated PC12 cells in the presence and the absence of CDP-Choline. Interestingly, CDP-Choline reduced MitoSox levels of 50μM Aβ treated PC12 cells. This situation suggests that CDP-Choline may have different roles in modulating mitochondrial dynamics under normal conditions and in the case of an injury, which suggests that CDP-Choline displays its protective effect under stressed conditions.

Moreover, recent publications urge on two different hypothesis concerning the aggregation process of Aβ peptide. One emphasizes Aβ injury is followed by soluble oligomers and defines fibrillar form of Aβ as inert while the other argues that fibrillar form of Aβ acts as the most damaging form. We used fibrillar form of $A\beta_{1\text{-}42}$ in our study and measured this structural formation by ThT-binding assay. This method needs additional quantification to characterize the fibrillar structure of Aβ peptides, since different forms of Aβ show different cellular effects. More specific quantification and characterization tools are required to discover the effects of both fibrillar and oligomeric forms of Aβ peptide (103, 127). Different results obtained from different concentrations of Aβ seen in our study may be explained by structural differences. Therefore, characterization of Aβ by different biochemical methods, like TEM, circular dichroism and AFM merits investigating (15).

In summary, CDP-Choline and Aβ-mediated injury affected autophagy protein levels and mitochondrial function of NGF-differentiated PC12 cells. Given the controversial roles of autophagy mechanism in neurodegeneration and unclear membrane sources for autophagosome formation, mechanism-based investigation of CDP-Choline on autophagic flux may contribute to enlighten its role in neurodegenerative diseases. It also may provide details about the mechanism of the neuroprotective effect of CDP-Choline with regard to find new therapeutic targets for the prevention and the treatment of neurodegenerative diseases.

5. REFERENCES

1. Abramovici H, Mojtabaie P, Parks RJ, Zhong XP, Koretzky GA, Topham MK, Gee SH. Diacylglycerol kinase zeta regulates actin cytoskeleton reorganization through dissociation of Rac1 from RhoGDI. Mol Biol Cell. 2009; 20(7):2049-2059

2. Adibhatla RM, Hatcher JF, Dempsey RJ. Citicoline: Neuroprotective mechanisms in cerebral ischemia. J Neurochem. 2002; 80(1):12-23

3. Alberts B, Johnson A, Lewis J, Raff M, Roberts K, Walter P. Molecular Biology of the Cell. 5th edition p813-840

4. Alegre F, Moragrega ÀB, Polo M, Marti-Rodrigo A, Esplugues JV, Blas-Garcia A, Apostolova N. Role of p62/SQSTM1 beyond autophagy: A lesson learned from drug-induced toxicity in vitro. Br J Pharmacol. 2018; 175(3):440-455

5. Anderson CJ, Kahl A, Qian L, Stepanova A, Starkov A, Manfredi G, Iadecola C, Zhou P. Prohibitin is a positive modulator of mitochondrial function in PC12 cells under oxidative stress. J Neurochem. 2018

6. Arenth PM, Russell KC, Ricker JH, Zafonte RD. CDP-Choline as a biological supplement during neurorecovery: A focused review. PM R. 2011; 3(6 Suppl 1):S123-131

7. Ariosa AR, Klionsky DJ. Autophagy core machinery: overcoming spatial barriers in neurons. J Mol Med (Berl). 2016; 94(11):1217-1227

8. Aufschnaiter A, Kohler V, Diessl J, Peselj C, Carmona-Gutierrez D, Keller W, Büttner S. Mitochondrial lipids in neurodegeneration. Cell Tissue Res. 2017; 367(1):125-140

9. Beckervordersandforth R. Mitochondrial metabolism-mediated regulation of adult neurogenesis. Brain Plast. 2017; 3(1):73-87

10. Benilova I, Karran E, De Strooper B. The toxic Aβ oligomer and Alzheimer's disease: An emperor in need of clothes. Nat Neurosci. 2012; 15(3):349-357

12. Bento CF, Renna M, Ghislat G, Puri C, Ashkenazi A, Vicinanza M, Menzies FM, Rubinsztein DC. Mammalian autophagy: How does it work?. Annu Rev Biochem. 2016; 85:685-713

13. Bertholet AM, Delerue T, Millet AM, Moulis MF, David C, Daloyau M, Arnauné-Pelloquin L, Davezac N, Mils V, Miquiel MC, Rojo M, Belenguer P. Mitochondrial fusion/fission dynamics in neurodegeneration and neuronal plasticity. Neurobiol Dis. 2016; 90:3-19

14. Briston T, Hicks AR. Mitochondrial dysfunction and neurodegenerative proteinopathies:mechanisms and prospects for therapeutic intervention. Biochem Soc Trans. 2018; pii:BST20180025

15. Bruggink KA, Müller M, Kuiperij HB, Verbeek MM. Methods for analysis of amyloid-β aggregates. J Alzheimers Dis. 2012; 28(4):735-58

16. Burté F, Carelli V, Chinnery PF, Yu-Wai-Man P. Disturbed mitochondrial dynamics and neurodegenerative disorders. Nat Rev Neurol. 2015; 11(1):11-24

17. Cai Q, Tammineni P. Alterations in mitochondrial quality control in Alzheimer's disease. Fron Cell Neurosci. 2016; 10:24

18. Chaban Y, Boekema EJ, Dudkina NV. Structures of mitochondrial oxidative phosphorylation supercomplexes and mechanisms for their stabilisation. Biochim Biophys Acta. 2017; 1837(4):418-426

19. Chadwick W, Brenneman R, Martin B, Maudsley S. Complex and multidimensional lipid raft alterations in a murine model of Alzheimer's disease. Int J Alzheimers Dis. 2010; 2010:604792

20. Chen Y, Dorn II GW. PINK-1 phosphorylated Mitofusin 2 is a Parkin receptor for culling damaged mitochondria. Science. 2013; 340(6131):471-475

21. Chong FP, Ng KY, Koh RY, Chye SM. Tau proteins and taupathies in Alzheimer's disease. Cell Mol Neurobiol. 2018; 38(5):965-980

22. Congdon EE, Sigurdsson EM. Tau-targeting therapies for Alzheimer disease. Nat Rev Neurol. 2018

23. Correia SC, Perry G, Moreira PI. Mitochondrial traffic jams in Alzheimer's disease-pinpointing the roadblocks. Biochim Biophys Acta. 2016; 1862(10):1909-1917

24. Cuervo AM, Wong E. Chaperone-mediated autophagy: Roles in disease and aging. Cell Res. 2014; 24(1):92-104

25. Dempsey RJ, Raghavendra Rao VL. Cytidinediphosphocholie treatment to decrease traumatic brain injury-induced hippocampal neuronal death, cortical contusion volume and neurological dysfunction in rats. J Neurosurg. 2003; 98(4):867-873

26. Deyts C, Thinakaran G, Parent AT. APP receptor? To be or not to be. Trends Pharmacol Sci. 2016; 37(5):390-411

27. Dikic I, Elazar Z. Mechanism and medical implications of mammalian autophagy. Nat Rev Mol Cell Biol. 2018; 19(6):349-364

28. Feng X, Liang N, Zhu D, Gao Q, Peng L, Dong H, Yue Q, Liu H, Bao L, Zhang J, Hao J, Gao Y, Yu X, Sun J. Resveratrol inhibits β-amyloid induced neuronal apoptosis through regulation of SIRT1-ROCK1 signaling pathway. PLoS One 2013; 8(3):e59888

29. Feng Y, He D, Yao Z, Klionsky DJ. The machinery of macroautophagy. Cell Res. 2014; 24(1):24-41

30. Fujikake N, Shin M, Shimizu S. Association between autophagy and neurodegenerative diseases. Front Neurosci. 2018; 12:255

31. Fujita N, Itoh T, Omori H, Fukuda M, Noda T, Yoshimori T. The Atg16L complex specifies the site of LC3 lipidation for membrane biogenesis in autophagy. Mol Biol Cell. 2008; 19(5):2092-2100

32. Funderburk SF, Marcellino BK, Yue Z. Cell "self-eating" (autophagy) mechanism in Alzheimer's disease. Mt Sinai J Med. 2010; 77(1):59-68

33. Gao J, Wang L, Liu J, Xie F, Su B, Wang X. Abnormalities of mitochondrial dynamics in neurodegenerative diseases. Antioxidants (Basel). 2017; 6(2).pii:E25

34. Gibellini F, Smith TK. The Kennedy pathway – de novo synthesis of phosphatidylethanolamine and phosphatidylcholine. IUBMB Life. 2010; 62(6):414-428

35. González-Pacheco H, Méndez-Dominiguez A, Hernández S, López-Marure R, Vazquez-Mellado MJ, Aguilar C, Rocha-Zavaleta L. Pre-conditioning with CDP-Choline attenuates oxidative stress-induced cardiac myocyte death in a hypoxia/reperfusion model. The Scientific World Journal 2014

36. Grieb P. Neuroprotective properties of citicoline: Facts, doubts and unresolved issues. CNS Drugs. 2014; 28(3):185-193

37. Grimm A, Eckert A. Brain aging and neurodegeneration: From a mitochondrial point of view. J Neurochem. 2017; 143(4):418-431

38. Gutiérrez-Fernández M, Rodriguez-Frutos B, Fuentes B, Vallejo-Cremades MT, Alvarez-Grech J, Expósito-Alcaide M, Díez-Tejedor E. CDP-Choline treatment induces brain plasticity markers expression in experimental animal stroke. Neurochem Int. 2012; 60(3):310-317

39. Han J, Qu Q, Qiao J, Zhang J. Vincamine alleviates amyloid-β 25-35 peptides-induced cytotoxicity in PC12 cells. Pharmacogn Mag. 2017; 13(49):123-128

40. Hang P, Zhao J, Su Z, Sun H, Chen T, Zhao L, Du Z. Choline inhibits ischemia-reperfusion-induced cardiomyocyte autophagy in rat myocardium by activating Akt/mTOR signalling. Cell Physiol Biochem. 2018; 45(5):2136-2144

41. Hara T, Nakamura K, Matsui M, Yamamato A, Nakahara Y, Suzuki-Migishima R, Yokoyama M, Mishima K, Saito I, Okano H, Mizushima N. Suppression of basal autophagy in neural cells causes neurodegenerative disease in mice. Nature. 2006; 441(7095):885-889

42. Hoppins S, Horner J, Song C, McCaffery JM, Nunnari J. Mitochondrial outer and inner membrane fusion requires a modified carrier protein. J Cell Biol. 2009; 184:569-581

43. Hsu P, Shi Y. Regulation of autophagy by mitochondrial phospholipids in health and diseases. Biochim Biophys Acta. 2017; 1862(1):114-129

44. Hu Y, Li XC, Wang ZH, Luo Y, Zhang X, Liu XP, Feng Q, Wang Q, Yue Z, Chen Z, Ye K, Wang JZ, Liu GP. Tau accumulation impairs mitophagy via increasing mitochondrial membrane potential and reducing mitochondrial Parkin. Oncotarget. 2016; 7(14):17356-68

45. Hung SY, Huang WP, Liou HC, Fu WM. Autophagy protects neuron from Abeta-induced cytotoxicity. Autophagy 2009; 5(4):502-510

46. Hüttemann M, Lee I, Samavati L, Yu H, Doan JW. Regulation of mitochondrial oxidative phosphorylation through cell signalling. Biochim Biophys Acta. 2007; 1773(12):1701-17204

47. Iqbal K, Liu F, Gong CX, Grundke-Iqbal I. Tau in Alzheimer disease and related taupathies. Curr Alzheimer Res. 2010; 7(8):656-664

48. Ittner A, Ittner LM. Dendritic tau in Alzheimer's disease. Neuron. 2018; 99(1):13-27

49. Iulia C, Ruxandra T, Costin LB, Liliana-Mary V. Citicoline- a neuroprotector with proven effects on glaucomatous disease. Rom J Opthalmol. 2017; 61(3):152-158

50. Kaur J, Debnath J. Autophagy at the crossroads of catabolism and anabolism. Nat Rev Mol Cell Biol. 2015; 16(8):461-472

51. Kawalec M, Boratyńska-Jasińska A, Beresewicz M, Dymkowska D, Zablocki K, Zablocka B. Mitofusin 2 deficiency affects energy metabolism and mitochondrial biogenesis in MEF cells. PLoS One. 2015; 10(7):e0134162

52. Kerr JS, Adriaanse BA, Greig NH, Mattson MP, Cader MZ, Bohr VA, Fang EF. Mitophagy and Alzheimer's disease: Cellular and molecular mechanisms. Trends Neurosci. 2017, 40(3):151-166

53. Kim JH, Choi BY, Kho AR, Lee SH, Jeong JH, Hong DK, Lee SH, Sohn M, Ryu OH, Choi MG, Suh SW. Acetylcholine precursor, citicoline (cytidine 5'-diphosphocholine), reduces hypoglycaemia-induced neuronal death in rats. J Neuroendocrinol. 2018; 30(1)

54. Kiriyama Y, Nochi H. The function of autophagy in neurodegenerative diseases. Int J Mol Sci. 2015; 16(11):26797-26812

55. Knævelsrud H, Simonsen A. Lipids in autophagy: Constituents, signalling molecules and cargo with relevance to disease. Biochim Biophys Acta. 2012; 1821(8):1133-1145

56. Komatsu M, Waguri S, Chiba T, Murata S, Iwata J, Tanida I, Ueno T, Koike M, Uchiyama Y, Kominami E, Tanaka K. Loss of autophagy in central nervous system causes neurodegeneration in mice. Nature. 2006; 441/7095):880-884

57. Lamb CA, Yoshimori T, Tooze SA. The autophagosome: Origins unknown, biogenesis complex. Nat Rev Mol Cell Biol. 2013; 14(12):759-74

58. Leuner K, Müller WE, Reichert AS. From mitochondrial dysfunction to amyloid beta formation: Novel insights into the pathogenesis of Alzheimer's disease. Mol Neurobiol. 2012; 46(1):186-193

59. Li X, Fang P, Mai J, Choi ET, Wang H, Yang XF. Targeting mitochondrial reactive oxygen species as novel therapy for inflammatory diseases and cancers. J Hematol Oncol. 2013; 6:19

60. Lilienbaum A. Relationship between the proteasomal system and autophagy. Int J Biochem Mol Biol. 2013; 4(1):1-26

61. Lionaki E, Markaki M, Palikaras K, Tavernarakis N. Mitochondria, autophagy and age-associated neurodegenerative diseases: New insight into a complex interplay. Biochim Biophys Acta. 2015; 1847(11)1412-1423

62. Logan A, Pell VR, Shaffer KJ, Evans C, Stanley NJ, Robb EL, Prime TA, Chouchani ET, Cochemé HM, Fearnley IM, Vidoni S, James AM, Porteous CM, Partridge L, Krieg T, Smith RA, Murphy MP. Assesing the mitochondrial membrane potential in cells and in vivo using targeted click chemistry and mass spectrometry. Cell Metab. 2016; 23(2):379-385

63. Lumkwana D, du Toit A, Kinnear C, Loos B. Autophagic flux control in neurodegeneration: Progress and precision targeting-where do we stand? Prog Neurobiol. 2017; 153:64-85

64. Manzoni C, Mamais A, Roosen DA, Dihanich S, Soutar MP, Plun-Favreau H, Bandopadhyay R, Hardy J, Tooze SA, Cookson MR, Lewis PA. mTOR independent regulation of macroautophagy by leucine rich repeat kinase 2 via Beclin-1. Sci Rep. 2016; 6:35106

65. Martinez-Vicente M. Neuronal mitophagy in neurodegenerative diseases. Front Mol Neurosci. 2017; 10:64

66. McNight NC, Zhong Y, Wold MS, Gong S, Phillips GR, Dou Z, Zhao Y, Heintz N, Zong WX, Yue Z. Beclin 1 is required for neuron viability and regulates endosome pathways via the UVRAG-VPS34 complex. PLoS Genet. 2014; 10(10):e1004626

67. Mejia EM, Hatch GM. Mitochondrial phospholipids: Role in mitochondrial function. J Bioenerg Biomemr. 2016; 48(2):99-112

68. Menzies FM, Fleming A, Caricasole A, Bento CF, Andrews SP, Ashkenazi A, Füllgrabe J, Jackson A, Jimenez Sanchez M, Karabiyik C, Licitra F, Lopez Ramirez A, Pavel M, Puri C, Renna M, Ricketts T, Schlotawa L, Vicinanza M, Won H, Zhu Y, Skidmore J, Rubinsztein DC. Autophagy and neurodegeneration: Pathogenic mechanisms and therapeutic opportunities. Neuron. 2017; 93(5):1015-1034

69. Metaxakis A, Ploumi C, Tavernarakis N. Autophagy in age-associated neurodegeneration. Cells. 2018; 7(5):37

70. Mitsuhashi S, Hatakeyama H, Karahashi M, Koumura T, Nonaka I, Hayashi YK, Noguchi S, Sher RB, Nakagawa Y, Manfredi G, Goto Y, Cox GA, Nishino I. Muscle choline kinase beta defect causes mitochondrial dysfunction and increased mitophagy. Hum Mol Genet. 2011; 20(19):3841-3851

71. Mizushima N. Autophagy: Process and function. Genes Dev. 2007; 21(22):2861-2873

72. Mizushima N, Komatsu N. Autophagy: Renovation of cells and tissues. Cell 2011; 147(4):728-742

73. Mizushima N, Yoshimori T. How to interpret LC3 immunoblotting. Autophagy 2007; 3(6):542-545

74. Mizushima N, Yoshimori T, Ohsumi Y. The role of Atg proteins in autophagosome formation. Annu Rev Cell Dev Biol. 2011; 27:107-132

75. Moretti, DV. (Ed), Update on Dementia, 2016:127-167

76. Nakamura S, Yoshimori T. New insights into autophagosome-lysosome fusion. J Cell Sci. 2017; 130(7):1209-1216

77. Nelson DL, Cox MM. Lehninger Principals of Biochemistry. 5th edition p527-760

78. Nguyen BY, Ruiz-Velasco A, Bui T, Collins L, Wang X, Liu W. Mitochondrial function in the heart: The insight into mechanisms and therapeutic potentials. Br J Pharmacol. 2018

79. Ni HM, Williams JA, Ding WX. Mitochondrial dynamics and mitochondrial quality control. Redox Biol. 2015; 4:6-13

80. Nixon RA. Autophagy in neurodegenerative disease: Friend, foe or turncoat? Trends Neurosci. 2006; 29(9):528-535

81. Nixon RA, Wegiel J, Kumar A, Yu WH, Peterhoff C, Catalfo A, Cuervo AM. Extensive involvement of autophagy in Alzheimer disease: An immune-electron microscopy study. J Neuropathol Exp Neurol. 2005; 64(2):113-122

82. Ntsapi C, Lumkwana D, Swart C, du Toit A, Loos B. New insights into autophagy dysfunction related to amyloid beta toxicity and neuropathology in Alzheimer's disease. Int ReV Cell Mol Biol. 2018; 336:321-361

83. Palikaras K, Daskalaki I, Markaki M, Tavernarakis N. Mitophagy and age-related pathologies: Development of new therapeutics by targeting mitochondrial turnover. Pharmacol Ther. 2017; 178:157-174

84. Penke B, Bogar F, Fülöp L. B-amyloid and the pathomechanisms of Alzheimer's disease: A comprehensive view. Molecules. 2017; 22(10).pii:E1692

85. Ploumi C, Daskalaki I, Tavernarakis N. Mitochondrial biogenesis and clearance: A balancing act. FEBS J. 2017; 284(2):183-195

86. Rodolfo C, Campello S, Cecconi F. Mitophagy in neurodegenerative diseases. Neurochem Int. 2018; 117:156-166

87. Rubinsztein DC, Bento CF, Deretic V. Therapeutic targeting of autophagy in neurodegenerative and infectious diseases. J Exp Med. 2015; 212(7):979:990

88. Sarkar S. Regulation of autophagy by mTOR-dependent and mTOR-independent pathways: Autophagy dysfunction in neurodegenerative diseases and therapeutic application of autophagic enhancers. Biochem Soc Trans. 2013; 41(5):1103-1130

89. Sazanov LA. A giant molecular proton pump: Structure and mechanism of respiratory complex I. Nat Rev Mol Cell Biol. 2015; 16(6):375-388

90. Scott I, Youle RJ. Mitochondrial fission and fusion. Essays Biochem. 2010; 47:85-9877

91. Sebatián D, Palacín M, Zorzano A. Mitochondrial dynamics: Coupling mitochondrial fitness with healthy aging. Trends Mol Med. 2017; 23(3):201-215

92. Sena LA, Chandel NS. Physiological roles of mitochondrial reactive oxygen species. Mol Cell. 2012; 48(2):158-167

93. Shatz O, Holland P, Elazar Z, Simonsen A. Complex relations between phospholipids, autophagy and neutral lipids. Trends Biochem Sci. 2016; 41(11):907-923

94. Shintani T, Klionsky DJ. Autophagy in health and disease: A double-edged sword. Science. 2004; 306(5698):990-995

95. Son JH, Shim JH, Kim KH, Ha JY, Han JY. Neuronal autophagy and neurodegenerative diseases. Exp Mol Med. 2012; 44(2):89-98

96. Sou Y, Waguri S, Ivata J, Ueno T, Fujimura T, Hara T, Sawada N, Yamada A, Mizushima N, Uchiyama Y, Kominami E, Tanaka K, Masaaki K. The Atg8 conjugation system is indispensable for proper development of autophagic isolation membranes in mice. Mol Bio Cell. 2008; 19(11):4762-4775.

97. Stavoe AKH, Holzbaur ELF. Axonal autophagy: Mini-review for autophagy in the CNS. Neurosci Lett. 2018; S0304-3940(18)30194-0

98. Stefanatos R, Sanz A. The rol of mitochondria ROS in the aging brain. FEBS Lett. 2018; 592(5):743-758

99. Sun L, Zhao M, Yang Y, Xue RQ, Yu XJ, Liu JK, Zang WJ. Acetylcholine attenuates hypoxia/reoxygenetion injury by inducing mitophagy through PINK1/Parkin signal pathway in H9c2 cells. J Cell Physiol. 2016; 231(5):1171-81

100. Tanida I, Minematsu-Ikeguchi N, Ueno T, Kominami E. Lysosomal turnover, but not a cellular level, of endogenous LC3 is a marker for autophagy. Autophagy. 2005; 1(2):84-91

101. Tekirdag K, Cuervo AM. Chaperone-mediated autophagy and endosomal microautophagy: Joint by chaperone. J Biol Chem. 2018; 293(15)Ç5414-5424

102. Testerink N, van der Sanden MH, Houweling M, Helms JB, Vaandrager AB. Depletion of phosphatidylcholine affects endoplasmic reticulum morphology and protein traffic at the Golgi complex. J Lipid Res. 2009; 50(11):2182-92

103. Tipping KW, van Oosten-Hawle P, Hewitt EW, Radford SE. Amyloid fibres: Inert end-stage aggregated or key players in disease? Trends Biochem Sci. 2015; 40(12):719-727

104. Towers CG, Thorburn A. Therapeutic targeting of autophagy. EBioMedicine. 2016; 14:15-23

105. Tönnies E, Trushina E. Oxidative stress, synaptic dysfunction and Alzheimer's disease. J Alzheimer Dis. 2017; 57(4):1105-1121

106. Villa RF, Ferrari F, Gorini A. Effect of CDP-Choline on age-dependent modificiations of energy- and glutamate- linked enzyme activities in synaptic and non-synaptic mitochondria from rat cerebral cortex. Neurochemistry International 2012; 61(8):1424-1432

107. Wai T, Langer T. Mitochondrial dynamics and metabolic regulation. Trends Endocrinol Metab. 2016; 27(2):105-117

108. Wang CS, Lee RK. Choline plus cytidine stimulate phopholipid production, and the expression and secretion of amyloid precursor protein in rat PC12 cells. Neuroscience Letters 2000; 283(1):25-28

109. Wang J, Chen GJ. Mitochondria as a therapeutic target in Alzheimer's disease. Genes&Diseases 2016; 3(3):220-227

110. Winslow AR, Rubinsztein DC. Autophagy in neurodegeneration and development. Biochim Biophys Acta. 2008; 1782(12):723-729

111. Wiravan E, Lippens S, Vanden Berghe T, Romagloni A, Fimia GM, Piacentini M, Vandenabeele P. Beclin1: A role in membrane dynamics and beyond. Autophagy 2012; 8(1):6-17

112. Wolfe DM, Lee JH, Kumar A, Lee S, Orenstein SJ, Nixon RA. Autophagy failure in Alzheimer's disease and the role of defective lysosomal acidification. Eur J Neurosci. 2013; 37(12):1949-1961

113. Wooten MW, Seibenhener ML, Mamidipudi V, Diaz-Meco MT, Barker PA, Moscat J. The atypical protein kinase C-interacting protein p62 is a scaffold for NF-kappaB activation by nerve growth factor. J Biol Chem. 2001; 276(11):7709-12

114. Wurtman RJ, Cansev M, Ulus IH. Choline and its products acetylcholine and phophatidylcholine. Handbook of Neurochemistry and Molecular Neurobiology p443-501

115. Wurtman RJ. How anticholinergic drugs might promote Alzheimer's disease: More amyloid-β and less phosphatidylcholine. J Alzheimers Dis. 2015; 46(4):983-987

116. Xu P, Li Z, Wang H, Zhang X, Yang Z. Triptolide inhibited cytotoxicity of differentiated PC12 cells induced by amlyoid-beta$_{25-35}$ via the autophagy pathway. PLoS One 2015; 10(11):e0142719

117. Xue Z, Zhang S, Huang L, He Y, Fang R. Upexpression of Beclin-1-dependent autophagy protects against beta-amyloid induced cell injury in PC12 cells. Journal of Molecular Neuroscience 2013; 51(1):180-186

118. Yang Z, Klionsky DJ. An overview of molecular mechanism of autophagy. Curr Top Microbiol Immunol. 2009; 335:1-32

119. Yang Z, Klionsky DJ. Eaten alive: A history of macroautophay. Nat Cell Biol. 2010; 12(9):814-822

120. Yang Z, Klionsky DJ. Mammalian autophagy: Core molecular machinery and signalling regulation. Curr Opin Cell Biol. 2010; 22(2):124-131

121. Yin Z, Pascual C, Klionsky DJ. Autophagy: Machinery and regulation. Microb Cell. 2016; 3(12):588-596

122. Youle RJ, van der Bliek AM. Mitochondrial fission, fusion and stress. Science. 2012; 337(6098):1062-1065

123. Yu L, Chen Y, Tooze SA. Autophagy pathway: Cellular and molecular mechanisms. Autophay. 2018; 14(2):207-215

124. Yu-shin S, Waguri S, Iwata J, Ueno T, Fujimura T, Hara T, Sawada N, Yamada A, Mizushima N, Uchiyama Y, Kominami E, Tanaka K, Komatsu M. The Atg8 conjugation system is indispensable for proper development of autophagic isolation membrane in mice. Mol Biol Cell. 2008; 19(11):4762-4775

125. Yu WH, Kumar A, Peterhoff C, Shapiro Kulnane L, Uchiyama Y, Lamb BT, Cuervo AM, Nixon RA. Autophagic vacuoles are enriched in amyloid precursor protein-secretase activities: Implications for β-amyloid peptide overproduction and localization in Alzheimer's disease. Int J Biochem. 2004; 36:2531-2540

126. Zazueta C, Buelna-Chontal M, Macías-López A, Román-Anguiano NG, González-Pacheco H, Pavón N, Springall R, Aranda-Frausto A, Bojalil R, Silva-Palacios A, Velázquez-Espejel R, Galvan Arzate S, Correrea F. CDP-Choline protects liver from ischemia/reperfusion injury preserving mitochondrial function and reducing oxidative stress. Liver Transpl. 2018

127. Zhang L, Trushin S, Christensen TA, Tripathi U, Hong C, Geroux RE, Howell KG, Poduslo JF, Trushina E. Differential effect of amyloid-beta peptides on mitochondrial

axonal trafficking depends on their state of aggregation and binding to the plasma membrane. Neurobiol Dis. 2018; 114:1-16

128. Zhang Q, Tamura Y, Roy M, Adachi Y, Iijima M, Sesaki H. Biosynthesis and roles of phospholipids in mitochondrial fusion, division and mitophagy. Cell Mol Life Sci. 2014; 71(19):3767-3778

129. Zorova LD, Papkov VA, Plotnikov EY, Silachev DN, Pevzner IB, Jankauskas SS, Babenko VA, Zorov SD, Balakireva AV, Juhaszova M, Sollott SJ, Zorov DB. Mitochondrial membrane potential. Anal Biochem. 2018; 552:50-59

CURRICULUM VITAE

Personal Information

Name	Begüm	**Surname**	Bilge
Place of birth	Istanbul	**Date of birth**	2.7.1990
Nationality	Turkey	**Telephone**	5334224156
E-mail	begumbilge7@gmail.com		

Education

	Institution	**Graduation Year**
BSc.	Sabanci University, Biological Sciences and Bioengineering	2014
High School	St. Joseph French High School, Istanbul	2009

Work Experience

Job Title	**Institution**	**Duration**
Erasmus+ Intern	Cancer Research UK, Edinburgh Center, Wilkinson Lab	March-June 2018
Intern	University of Virginia School of Medicine, Kedes Lab	June-Sept 2013

Languages

	Reading	**Speaking**	**Writing**
English	Very good	Very good	Very good
French	Good	Good	Good

Exams

	Score
ALES	70
IELTS	7,5

Computer Skills

Program	**Skill degree**
Microsoft Office	Very good
C++	Basic